Supporting Information

1,2-Insertion Reactions of Alkynes into Ge–C Bonds of Arylbromogermylenes

Tomohiro Sugahara,[a] Arturo Espinosa Ferao,[b] Alicia Rey Planells,[b] Jing-Dong Guo,[c] Shin Aoyama,[d] Kazunobu Igawa,[e] Katsuhiko Tomooka,[e] Takahiro Sasamori,[c]* Daisuke Hashizume,[f] Shigeru Nagase,[g] and Norihiro Tokitoh[a]

[a] Institute for Chemical Research, Kyoto University, Gokasho, Uji, Kyoto 611-0011, Japan.

[b] Deparamento de Química Orgánica, Universidad de Murcia, Campus de Espinardo, 30100 Murcia, Spain.

[c] Graduate School of Natural Sciences, Nagoya City University, Yamanohata 1, Mizuho-cho, Mizuho-ku, Nagoya, Aichi 467-8501, Japan.

[d] Department of Molecular and Material Sciences, Kyushu University, Kasuga-koen 6-1, Kasuga, Fukuoka 816-8580, Japan.

[e] Institute for Materials Chemistry and Engineering, Kyushu University, Kasuga-koen 6-1, Kasuga, Fukuoka 816-8580, Japan.

[f] RIKEN Center for Emergent Matter Science (CEMS), 2-1 Hirosawa, Wako, Saitama 351-0198, Japan.

[g] Fukui Institute for Fundamental Chemistry, Kyoto University, Sakyo-ku, Kyoto 606-8103, Japan.

E-mail: sasamori@nsc.nagoya-cu.ac.jp

Fax: +81-52-872-5820

1. General Remarks.

All manipulations were carried out under an argon atmosphere using either Schlenk line techniques or glove boxes. All solvents were purified by standard methods and/or the Ultimate Solvent System, Glass Contour Company.[S1] Remaining trace amounts of water and oxygen in the solvents were thoroughly removed by bulb-to-bulb distillation from potassium mirror prior to use. ^{1}H and ^{13}C NMR spectra were measured on a JEOL JNM-ECA600 (^{1}H: 600 MHz, ^{13}C: 151 MHz) in the Joint Usage/Research Center (JURC, Institute for Chemical Research, Kyoto University) or on a JEOL AL-300 spectrometer (^{1}H: 300 MHz, ^{13}C: 75 MHz). Signals arising from residual C_6D_5H (7.15 ppm) in the C_6D_6 was used as an internal standard for the ^{1}H NMR spectra, and that of C_6D_6 (128.0 ppm) for the ^{13}C NMR spectra. Multiplicity of signals in ^{13}C NMR spectra was determined by DEPT technique. High-resolution mass spectra (HRMS) were obtained from a Bruker micrOTOF focus-Kci mass spectrometer (DART). UV-vis spectra were recorded on a Shimadzu UV-2600 UV-vis spectrophotometer. All melting points were determined on a Büchi Melting Point Apparatus M-565 and are uncorrected. Elemental analyses were carried out at the Microanalytical Laboratory (Institute for Chemical Research of Kyoto University or RIKEN Center for Emergent Matter Science (CEMS)). 1,2-dibromodigermene **1**, cycloalkyne **5a**, and 1,2-dibromodisilene **12** were prepared according to the reported procedures.[S2]

2. Experimental Section

Reaction of 1,2-dibromodigermene 1 with 3-hexyne:

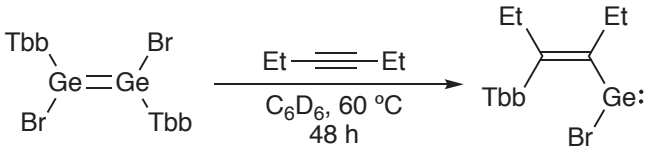

1 **3**

To a C_6D_6 solution (0.5 mL) of 1,2-dibromodigermene **1** (21.2 mg, 17.6 μmol as dimer) in a 5ϕ *J*-young NMR tube was added 3-hexyne (3.5 mg, 42.6 μmol, 2.4 equiv.). The reaction mixture was heated at 60 ºC for 48 h, and then the color of the yellow solution gradually changed to pale yellow. After removal of residual 3-hexyne and solvent under reduced pressure, the residue was recrystallized from hexane to afford bromovinylgermylene **3** as yellow crystals in 95% yield (23.0 mg, 33.6 μmol).

3: yellow crystals, mp 129.4 °C (dec.); ^{1}H NMR (300 MHz, 298 K, C_6D_6) δ 0.05 (s, 18H, CH(Si*Me*$_3$)$_2$), 0.08 (s, 18H, CH(Si*Me*$_3$)$_2$), 1.24 (t, 3H, *J* = 7.5 Hz, CH_2CH_3), 1.28 (s, 9H, C(*Me*)$_3$), 1.34 (t, 3H, *J* = 7.5 Hz, CH_2CH_3), 1.88 (s, 2H, C*H*Si), 2.43 (q, 2H, *J* = 7.5 Hz, CH_2CH_3), 3.16 (q, 2H, *J* = 7.5 Hz, CH_2CH_3), 6.86 (s, 2H, Ar*H*); ^{13}C NMR (75 MHz, 298 K, C_6D_6) δ 1.33 (q), 2.19 (q), 14.42 (q), 15.92 (q), 25.45 (t), 26.15 (d), 29.41 (t), 31.30 (q), 34.35 (s), 121.90 (d), 135.96 (s), 144.50 (s), 150.00 (s), 161.38 (s), 179.43 (s). UV−vis (*n*-hexane) λ_{max} (nm, ε) = 451 (br, 500). Anal. calcd for $C_{30}H_{59}BrGeSi_4$: C, 52.63; H, 8.69. found: C, 52.71; H, 8.94. MS (DART-TOF, positive mode): *m*/*z* calcd for $C_{30}H_{60}{}^{79}Br^{74}GeSi_4$ 685.2167 ($[M+H]^+$), found 685.2082 ($[M+H]^+$).

Reaction of 1,2-dibromodigermene 1 with cycloalkyne 5a:

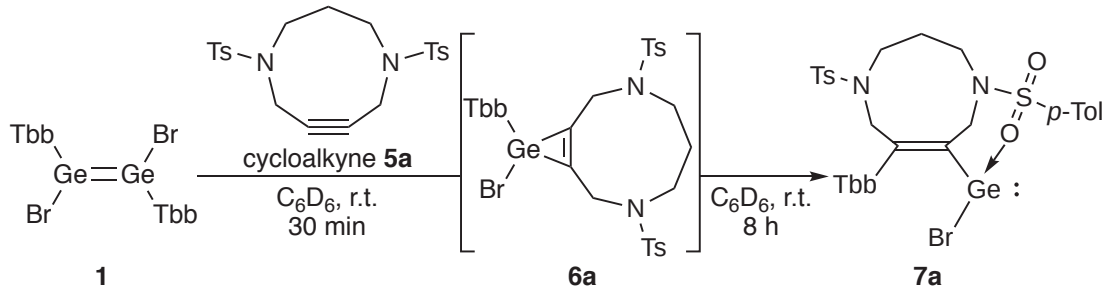

To a C_6D_6 solution (0.5 mL) of 1,2-dibromodigermene **1** (10.5 mg, 8.7 μmol as dimer) in a 5ϕ *J*-young NMR tube was added cycloalkyne **5a** (7.3 mg, 16.9 μmol, 2 equiv.). After 30 min, the signals of **1** disappeared and those for [1+2]cycloadduct **6a** were observed in the ^{1}H NMR spectra without any signal of a by-product. After 8 h, the quantitative formation of bromovinylgermylene **7a** was observed along with disappearance of **6a**. All volatiles were removed under reduced pressure at room temperature and the residue was washed with hexane to afford **7a** in quantitative yield (17.7 mg, 16.8 μmol).

6a: colorless powder; ^{1}H NMR (300 MHz, 298 K, C_6D_6) δ 0.25 (s, 36H, CH(Si*Me*$_3$)$_2$), 1.26 (s, 9H, C(*Me*)$_3$), 1.93 (s, 6H, Ar*Me*), 2.00–2.07 (m, 2H, $CH_2CH_2CH_2$), 2.55 (s, 2H, C*H*Si), 3.02–3.10 (m, 2H, NCH_2CH_2), 3.22–3.31 (m, 2H, NCH_2CH_2), 4.23 (d, 2H, *J* = 16.8 Hz, C=CCH_2N), 4.62 (d, 2H, *J* = 16.8 Hz, C=CCH_2N), 6.88 (d, 4H, *J* = 8.1 Hz, *p*Tol*H*), 6.96 (s, 2H, Ar*H*) , 7.76 (d, 2H, *J* = 8.1 Hz, *p*Tol*H*); ^{13}C NMR (75 MHz, 298 K, C_6D_6) δ 0.75 (q), 21.12 (q), 29.73 (t), 31.13 (q), 34.19 (d), 34.62 (s), 49.18 (t), 50.68 (t), 121.04 (d), 129.83 (d), 130.03 (d), 135.42 (s), 136.25 (s), 143.11 (s), 148.74 (s), 153.45 (s), 159.44 (s).

7a: colorless crystals, mp 156.7−157.7 °C; ^{1}H NMR (300 MHz, 298 K, C_6D_6) δ –0.27 (s, 9H, CH(Si*Me*$_3$)$_2$), 0.26 (s, 9H, CH(Si*Me*$_3$)$_2$), 0.34 (s, 9H, CH(Si*Me*$_3$)$_2$), 0.53 (s, 9H, CH(Si*Me*$_3$)$_2$), 1.26 (s, 9H, C(*Me*)$_3$), 1.88 (s, 3H, Ar*Me*), 1.89 (s, 3H, Ar*Me*), 2.00 (s, 1H, C*H*Si), 2.10–2.21 (m, 1H, $CH_2CH_2CH_2$), 2.39 (s, 1H, C*H*Si), 2.51–2.60 (m, 1H, $CH_2CH_2CH_2$), 3.10–3.43 (m, 3H, NCH_2CH_2), 3.27 (d, 1H, *J* = 16.8 Hz, C=CCH_2N), 4.04–4.14 (m, 1H, NCH_2CH_2), 4.92 (d, 1H, *J* = 14.7 Hz, C=CCH_2N), 5.16 (d, 1H, *J* = 16.8 Hz, C=CCH_2N), 5.50 (d, 1H, *J* = 14.7 Hz, C=CCH_2N), 6.78–6.84 (m, 5H, Ar*H*+*p*Tol*H*), 6.96 (s, 1H, Ar*H*) , 7.72 (d, 2H, *J* = 8.1 Hz, *p*Tol*H*), 8.03 (d, 2H, *J* = 8.1 Hz, *p*Tol*H*); ^{13}C NMR (151 MHz, 298 K, C_6D_6) δ 1.28 (q), 2.03 (q), 2.59 (q), 3.87 (q), 21.04 (q), 21.10 (q), 24.18 (d), 25.79 (d), 31.05 (t), 31.15 (q), 34.29 (s), 46.18 (t), 49.84 (t), 51.06 (t), 57.64 (t), 122.86 (d), 123.84 (d), 127.88 (d), 128.44 (d), 130.02 (d), 130.07 (d), 132.03 (s), 132.68 (s), 134.39 (s), 143.06 (s), 143.10 (s), 143.87 (s), 144.21 (s), 145.81 (s), 149.70 (s), 163.87 (s). Anal. calcd for $C_{45}H_{73}BrGeN_2O_4S_2Si_4$: C, 52.22; H, 7.11; N, 2.71. found: C, 52.93; H, 7.16; N, 2.68. MS (DART-TOF, positive mode): *m*/*z* calcd for $C_{45}H_{73}{}^{79}Br^{74}GeN_2O_4S_2Si_4$ 1034.2484 ([M]$^+$), found 1034.2554 ([M]$^+$).

* Melting point, Elemental analysis and Mass spectroscopy of **6a** could not be measure due to its facile conversion at room temperature.

Synthesis of *N*Ts,*N*′Ts-6,6-dimethyl-4,8-diazacyclononyne 5b:

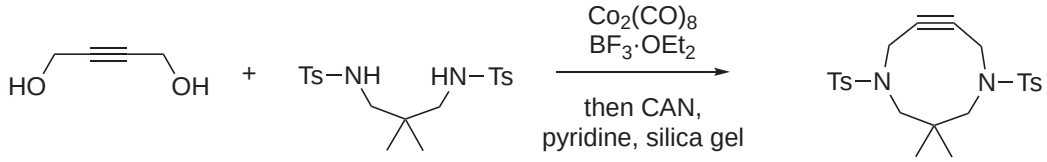

A **5b**

To a solution of 2-butyne-1,4-diol (155 mg, 1.80 mmol) in CH_2Cl_2 (60 mL) was added $Co_2(CO)_8$ (641 mg, 1.88 mmol) at 30 °C. After the mixture had been stirred at that temperature for 1 h, an additional CH_2Cl_2 (150 mL), precursor **A** (616 mg, 1.50 mmol) and BF_3·OEt_2 (754 μL, 6.00 mmol) were sequentially added and stirred at 30 °C for 3 h. Silica gel (12.6 g) and ceric ammonium nitrate (CAN: 2.47 g, 4.50 mmol) were sequentially added and stirred at that temperature for 3 h, then pyridine (484 μL, 6.00 mmol) and aminopropylated silica gel (15.0 g) were added to the mixture. After the mixture had been stirred at that temperature for 1 h, the mixture was filtered through filter paper using AcOEt as an eluent, and the filtrate was concentrated under reduced pressure.

The residue was purified by silica gel column chromatography (eluate: chloroform) to afford **5b** as stable colorless crystals (252 mg, 547 mmol, 36%).

5b: colorless crystals, mp 210.0–212.0 °C: ^{1}H NMR (300 MHz, $CDCl_3$, r.t.): δ 1.16 (s, 6H, C*Me*), 2.43 (s, 6H, CH_2CMe_2CH_2), 3.10 (s, 4H, CH_2CMe_2CH_2), 3.65 (s, 4H, C=CCH_2N), 7.33 (d, 4H, *J* = 8.1 Hz, *p*Tol*H*), 7.64 (d, 4H, *J* = 8.1 Hz, *p*Tol*H*); ^{13}C NMR (75 MHz, $CDCl_3$, r.t.): δ 21.60 (q), 26.74 (q), 38.24 (s), 41.46 (t), 55.19 (t), 86.77 (s), 128.00 (d), 129.94 (d), 133.34 (s), 144.15 (s). MS (DART-TOF, positive mode): *m*/*z* calcd for $C_{23}H_{28}N_2O_4S_2$: 461.1563 ([M+H]$^+$); found: 460.1575 ([M+H]$^+$).

Reaction of 1,2-dibromodigermene 1 with cycloalkyne 5b at room temperature:

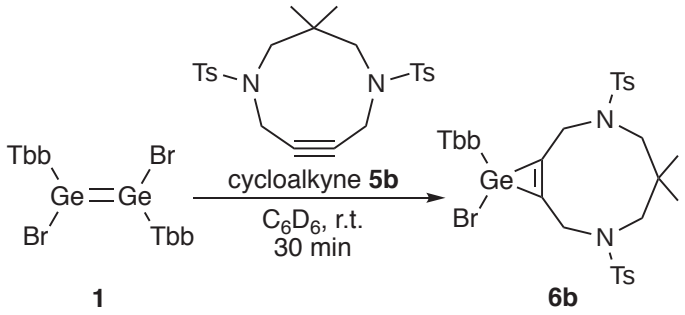

1 **6b**

To a C_6D_6 solution (0.5 mL) of 1,2-dibromodigermene **1** (8.9 mg, 8.7 μmol as dimer) in a 5ϕ *J*-young NMR tube was added cycloalkyne **5b** (7.3 mg, 16.9 μmol, 2 equiv.). After 30 min, the signals of **1** disappeared and those for [1+2]cycloadduct **6b** were observed in the ^{1}H NMR spectra without any signal of a by-product. After removal of residual solvent under reduced pressure, the residue was recrystallized from benzene to **6b** as colorless crystals in 98% yield (15.5 mg, 14.6 μmol).

6b: colorless crystals, 82.1 °C (dec.); ^{1}H NMR (300 MHz, 298 K, C_6D_6) δ 0.29 (s, 36H, CH(Si*Me*$_3$)$_2$), 0.94 (s, 3H, C*Me*), 1.23 (s, 3H, C*Me*), 1.29 (s, 9H, C(*Me*)$_3$), 1.93 (s, 6H, Ar*Me*), 2.67 (s, 2H, C*H*Si), 2.88 (d, 2H, *J* = 15.0 Hz, CH_2CMe_2CH_2), 3.61 (d, 2H, *J* = 15.0 Hz, CH_2CMe_2CH_2), 4.34 (d, 2H, *J* = 16.8 Hz, C=CCH_2N), 4.88 (d, 2H, *J* = 16.8 Hz, C=CCH_2N), 6.86 (d, 4H, *J* = 8.1 Hz, *p*Tol*H*), 7.03 (s, 2H, Ar*H*) , 7.75 (d, 2H, *J* = 8.1 Hz, *p*Tol*H*); ^{13}C NMR (75 MHz, 298 K, C_6D_6) δ 0.81 (q), 21.08 (q), 25.99 (q), 28.24 (q), 31.17 (q), 33.79 (d), 34.63 (s), 37.93 (s), 50.45 (t), 60.83 (t), 121.10 (d), 127.33 (d), 129.85 (d), 135.69 (s), 137.62 (s), 142.93 (s), 148.78 (s), 153.30 (s), 161.01 (s). Anal. calcd for $C_{47}H_{77}BrGeN_2O_4S_2Si_4$: C, 53.10; H, 7.30; N, 2.64. found: C, 53.87; H, 7.23; N, 2.19. MS (DART-TOF, positive mode): *m*/*z* calcd for $C_{47}H_{78}{}^{79}Br^{74}GeN_2O_4S_2Si_4$ 1063.2875 ([M+H]$^+$), found 1063.2856 ([M+H]$^+$).

Reaction of 1,2-dibromodigermene 1 with cycloalkyne 5b at 60 ºC:

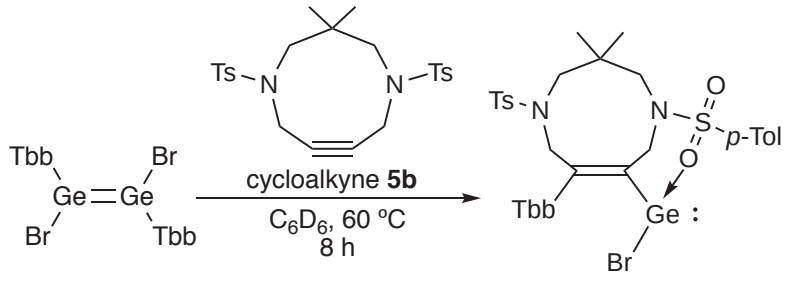

1 **7b**

To a C_6D_6 solution (0.5 mL) of 1,2-dibromodigermene **1** (8.8 mg, 7.3 μmol as dimer) in a 5ϕ *J*-young NMR tube was added cycloalkyne **5b** (6.7 mg, 14.5 μmol, 2 equiv.). After 30 min, the signals of **1** disappeared and those for [1+2]-cycloadduct **6b** were observed in the ^{1}H NMR spectra without any signal of a by-product. The reaction mixture was heated at 60 ºC for 12 h, and then the color of the yellow solution gradually changed to colorless. After removal of solvent under reduced pressure, the residue was washed with hexane to afford **7b** in 94% yield (14.0 mg, 13.2 μmol).

7b: colorless crystals, mp 182.0−183.0 °C; ^{1}H NMR (300 MHz, 298 K, C_6D_6) δ –0.13 (s, 9H, CH(Si*Me*$_3$)$_2$), 0.28 (s, 9H, CH(Si*Me*$_3$)$_2$), 0.37 (s, 9H, CH(Si*Me*$_3$)$_2$), 0.51 (s, 9H, CH(Si*Me*$_3$)$_2$), 1.27 (s, 9H, C(*Me*)$_3$), 1.32 (s, 3H, C*Me*), 1.36 (s, 3H, C*Me*), 1.86 (s, 3H, Ar*Me*), 1.88 (s, 3H, Ar*Me*), 2.15 (br, s, 1H, C*H*Si), 2.43 (br, s, 1H, C*H*Si), 3.11–3.55 (m, 5H, C*H*$_2$CMe$_2$CH$_2$+C=CC*H*$_2$N), 5.15 (d, 1H, *J* = 16.2 Hz, C*H*$_2$CMe$_2$CH$_2$), 5.30 (d, 1H, *J* = 14.4 Hz, C=CC*H*$_2$N), 5.63 (d, 1H, *J* = 14.4 Hz, C=CC*H*$_2$N), 6.79 (d, 2H, *J* = 8.1 Hz, *p*Tol*H*), 6.80 (d, 2H, *J* = 8.1 Hz, *p*Tol*H*), 6.85 (s, 1H, Ar*H*), 6.98 (s, 1H, Ar*H*), 7.72 (d, 2H, *J* = 8.1 Hz, *p*Tol*H*), 8.03 (d, 2H, *J* = 8.1 Hz, *p*Tol*H*); ^{13}C NMR (75 MHz, 298 K, C_6D_6) δ 1.63 (q), 2.19 (q), 2.67 (q), 3.98 (q), 21.00 (q), 21.13 (q), 24.19 (d), 25.92 (d), 26.20 (q), 30.48 (q), 31.19 (q), 34.30 (s), 38.49 (s), 49.67 (t), 58.64 (t), 60.78 (t), 60.97 (t), 122.95 (d), 123.54 (d), 127.85 (d), 128.58 (d), 129.90 (d), 130.01 (d), 130.58 (s), 133.44 (s), 134.38 (s), 142.72 (s), 143.03 (s), 143.81 (s), 144.33 (s), 146.28 (s), 149.68 (s), 162.29 (s). Anal. calcd for $C_{47}H_{77}BrGeN_2O_4S_2Si_4$: C, 53.10; H, 7.30; N, 2.64. found: C, 52.21; H, 7.27; N, 2.17. MS (DART-TOF, positive mode): *m*/*z* calcd for $C_{47}H_{78}{}^{79}Br^{74}GeN_2O_4S_2Si_4$ 1063.2875 ([M+H]$^+$), found 1063.2887 ([M+H]$^+$).

Reaction of 1,2-dibromodisilene 8 with 3-hexyne:

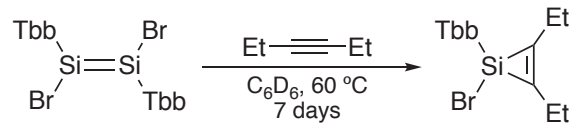

12 **14**

To a C_6D_6 solution (0.5 mL) of 1,2-dibromodisilene **12** (11.8 mg, 10.6 μmol as dimer) in a 5ϕ *J*-young NMR tube was added 3-hexyne (4.8 mg, 58.4 μmol, 5.5 equiv.). The reaction mixture was heated at 60 ºC for 7 days, and then the color of the yellow solution gradually changed to pale yellow. After removal of residual 3-hexyne and solvent under reduced pressure, the residue was recrystallized from hexane to afford [1+2]cycloadduct **14** as colorless crystals in 97% yield (13.1 mg, 20.5 μmol).

14: colorless crystals, mp 123.0 °C (dec.); ^{1}H NMR (300 MHz, 298 K, C_6D_6) δ 0.21 (s, 36H, CH(Si*Me*$_3$)$_2$), 1.22 (t, 6H, *J* = 7.5 Hz, CHC*H*$_3$), 1.28 (s, 9H, C(*Me*)$_3$), 2.46 (dq, 2H, *J* = 14.7, 7.5 Hz, C*H*CH$_3$), 2.70 (dq, 2H, *J* = 14.7, 7.5 Hz, C*H*CH$_3$), 2.70 (s, 2H, C*H*Si), 6.93 (s, 2H, Ar*H*); ^{13}C NMR (75 MHz, 298 K, C_6D_6) δ 0.78 (q), 13.23 (q), 22.62 (t), 31.15 (q), 32.39 (d), 34.55 (s), 120.79 (d), 131.38 (s), 149.48 (s), 152.92 (s), 161.95 (s); ^{29}Si NMR (59 MHz, 298 K, C_6D_6) δ–99.37 (*Si*Br), 2.78 (*Si*Me$_3$). Anal. calcd for $C_{30}H_{59}BrSi_5$: C, 56.29; H, 9.29. found: C, 55.54; H, 9.49. MS (DART-TOF, positive mode): *m*/*z* calcd for $C_{30}H_{60}{}^{79}BrSi_5$ 639.2725 ([M+H]$^+$), found 639.2711 ([M+H]$^+$).

Reaction of 1,2-dibromodisilene 8 with cycloalkyne 5a:

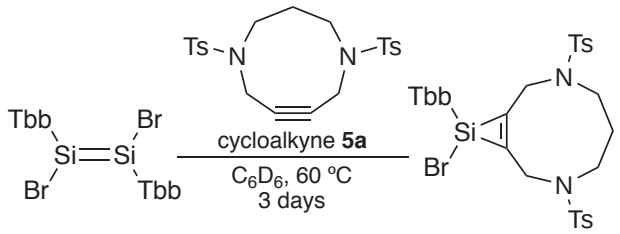

12 **16**

To a C_6D_6 solution (0.5 mL) of 1,2-dibromodisilene **12** (29.6 mg, 26.5 μmol as dimer) in a 5ϕ *J*-young NMR tube was added cycloalkyne **5a** (10.5 mg, 24.3 μmol, 0.9 equiv.). The reaction mixture was heated at 60 ºC for 3 days, and then the color of the yellow solution gradually changed to pale yellow. After removal of solvent under reduced pressure, the residue was recrystallized from hexane to afford [1+2]cycloadduct **16** as colorless crystals in 88% yield (21.3 mg, 21.5 μmol).

16: colorless crystals, mp 93.3–94.3 °C; ^{1}H NMR (300 MHz, 298 K, C_6D_6) δ 0.26 (s, 36H, CH(Si*Me*$_3$)$_2$), 1.28 (s, 9H, C(*Me*)$_3$), 1.93 (s, 6H, Ar*Me*), 2.02–2.10 (m, 2H, $CH_2CH_2CH_2$), 2.58 (s, 2H, C*H*Si), 3.04–3.28 (m, 4H, NCH_2CH_2), 4.21 (d, 2H, *J* = 16.5 Hz, C=CCH_2N), 4.55 (d, 2H, *J* = 16.5 Hz, C=CCH_2N), 6.87 (d, 4H, *J* = 8.4 Hz, *p*Tol*H*), 6.96 (s, 2H, Ar*H*) , 7.76 (d, 4H, *J* = 8.4 Hz, *p*Tol*H*); ^{13}C NMR (75 MHz, 298 K, C_6D_6) δ 0.87 (q), 21.10 (q), 29.92 (t), 31.11 (q), 33.08 (d), 34.62 (q), 49.32 (t), 50.32 (t), 120.77 (d), 127.70 (d), 129.80 (d), 130.05 (s), 136.19 (s), 143.06 (s), 149.87 (s), 153.61 (s), 158.92 (s); ^{29}Si NMR (59 MHz, 298 K, C_6D_6) δ–99.54 (*Si*Br), 2.96 (*Si*Me$_3$). Anal. calcd for $C_{45}H_{72}BrN_2O_4S_2Si_5$: C, 54.57; H, 7.43; N, 2.83. found: C, 54.91; H, 7.63; N, 2.08.

MS (DART-TOF, positive mode): *m*/*z* calcd for $C_{45}H_{73}{}^{79}BrN_2O_4S_2Si_5$ 989.3120 ($[M+H]^+$), found 989.3171 ($[M+H]^+$).

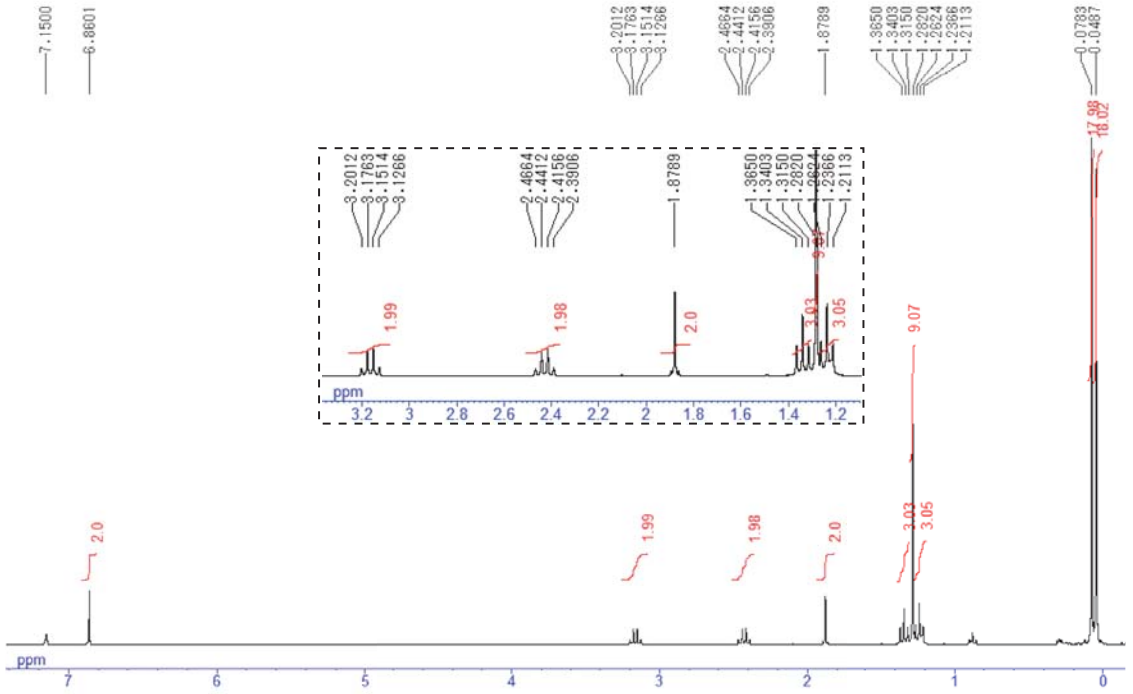

Figure S1. ^{1}H NMR spectrum of **3** in C_6D_6.

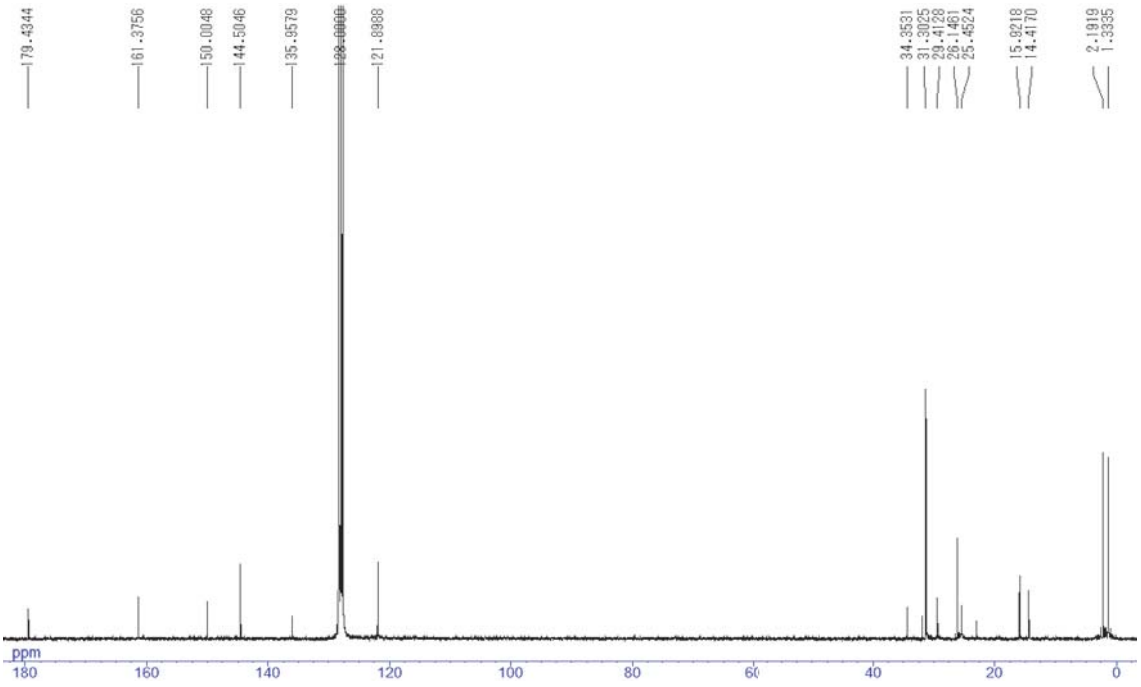

Figure S2. ^{13}C NMR spectrum of **3** in C_6D_6.

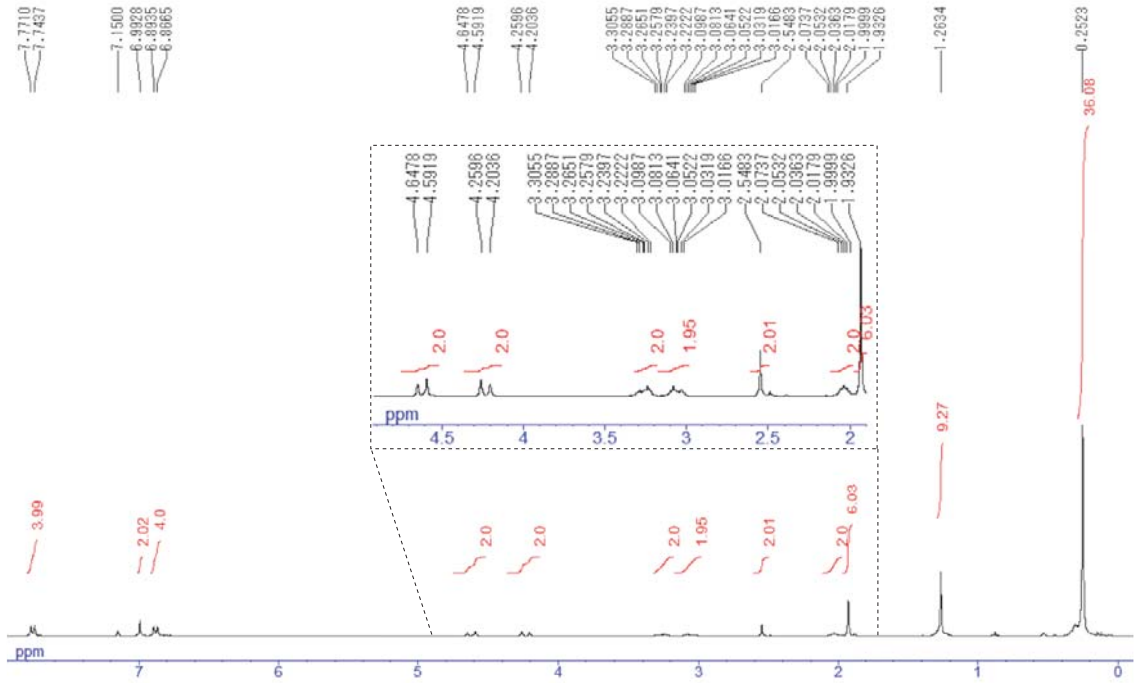

Figure S3. ^{1}H NMR spectrum of **6a** in C_6D_6.

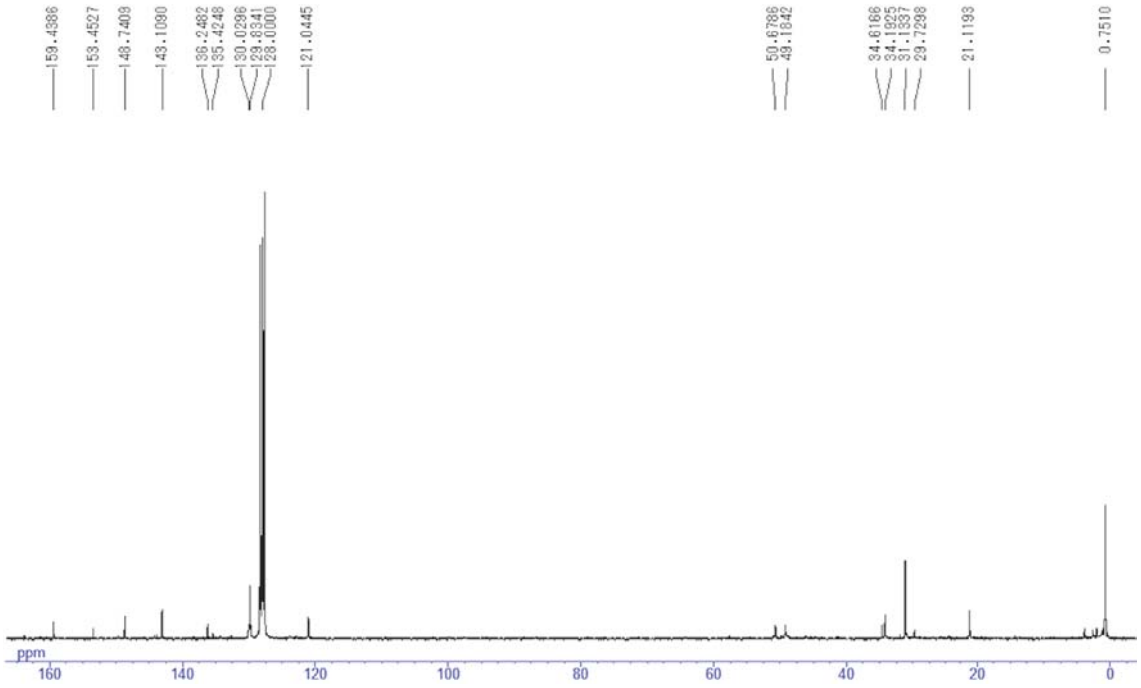

Figure S4. ^{13}C NMR spectrum of **6a** in C_6D_6.

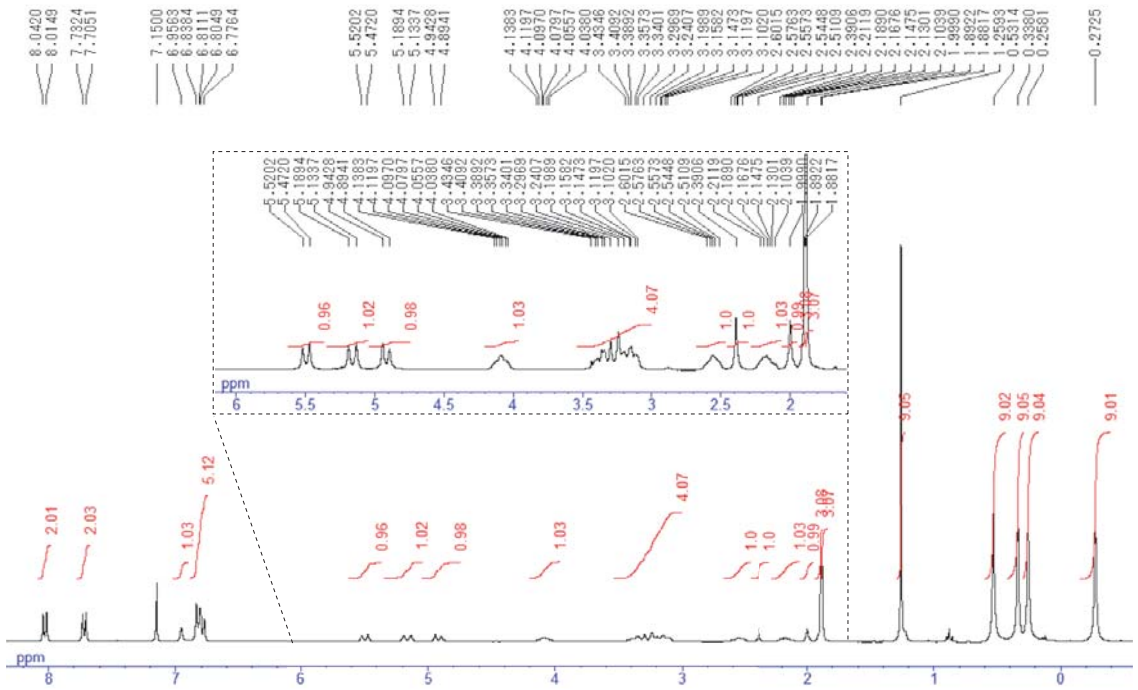

Figure S5. ^{1}H NMR spectrum of **7a** in C_6D_6.

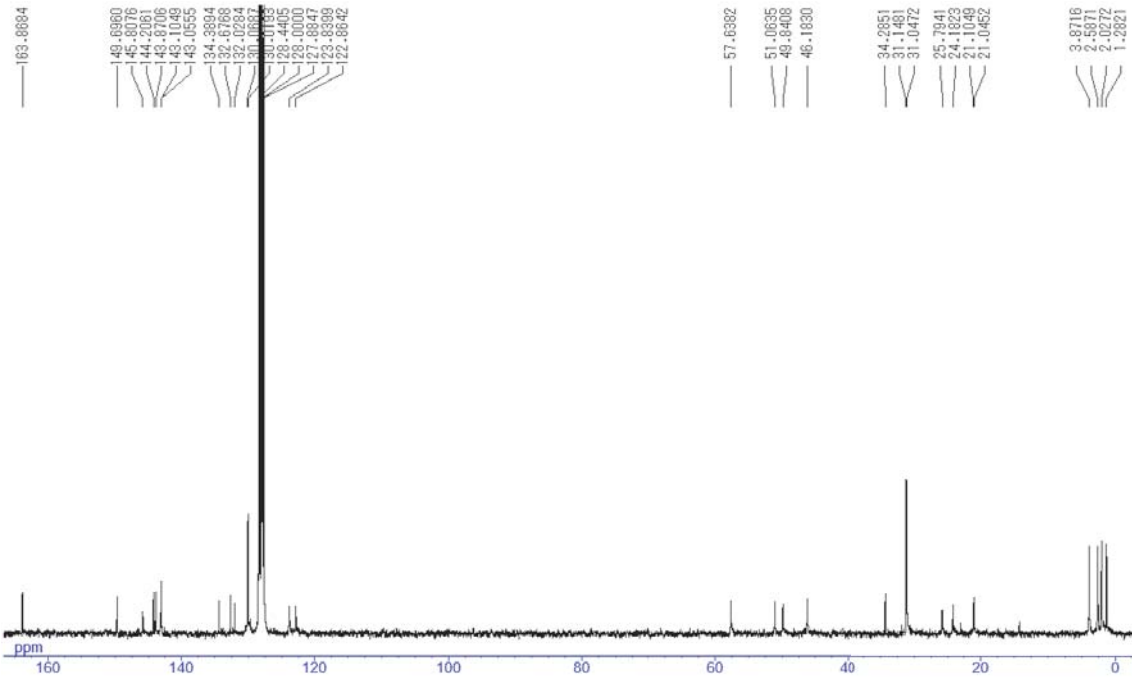

Figure S6. ^{13}C NMR spectrum of **7a** in C_6D_6.

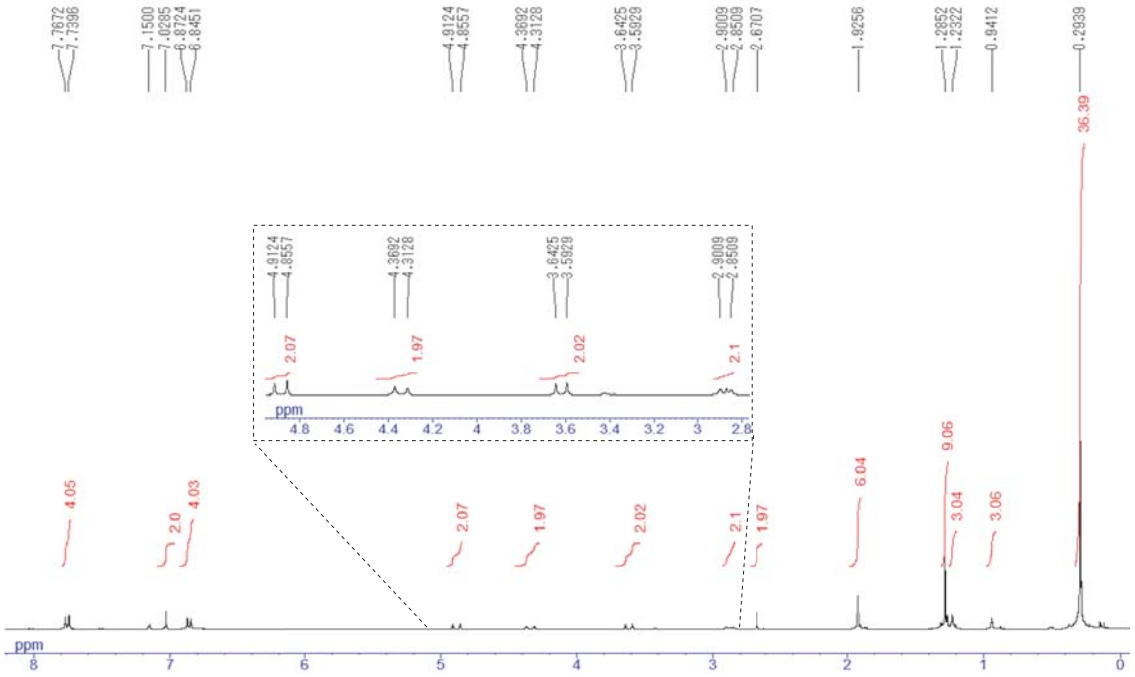

Figure S7. ^{1}H NMR spectrum of **6b** in C_6D_6.

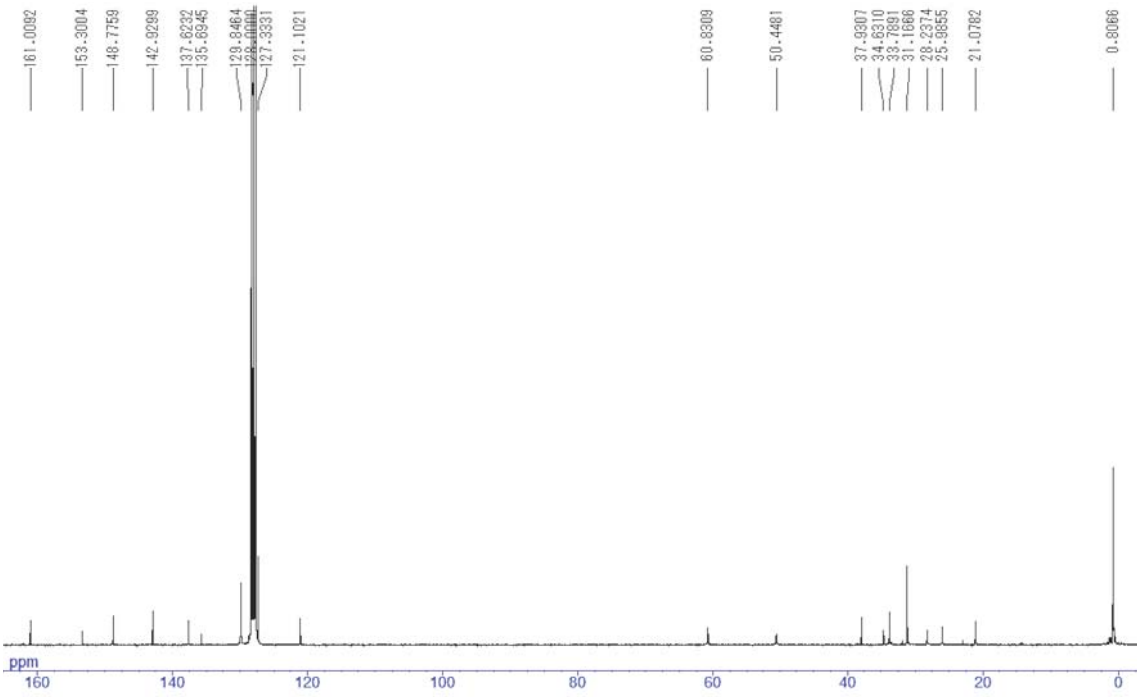

Figure S8. ^{13}C NMR spectrum of **6b** in C_6D_6.

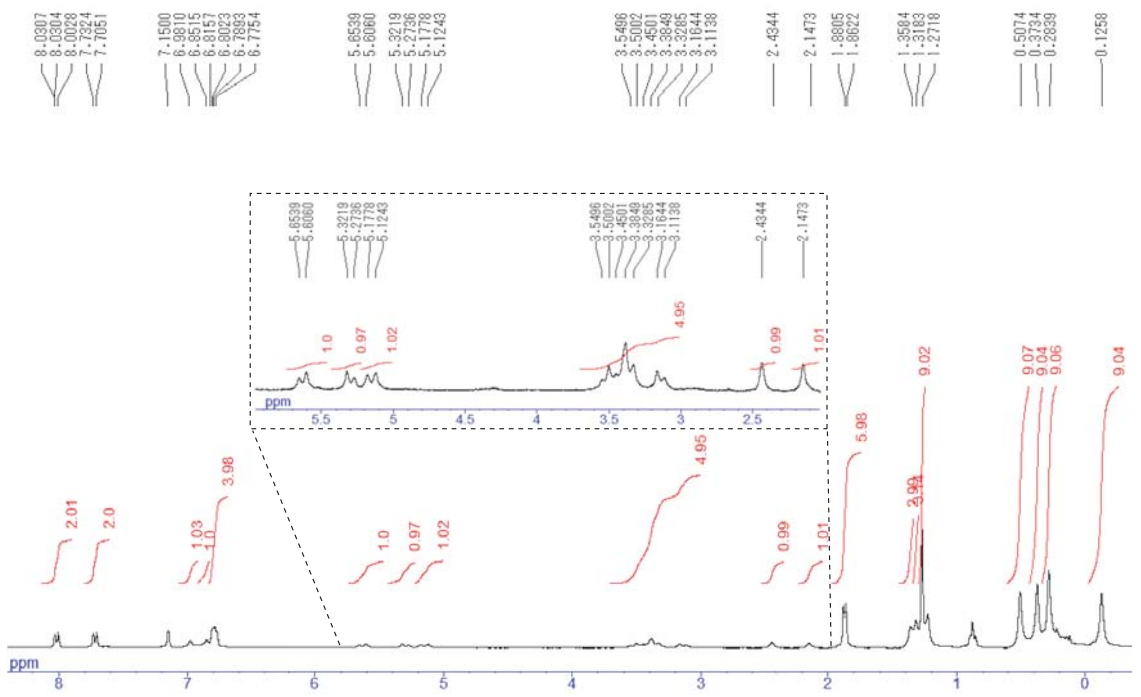

Figure S9. ^{1}H NMR spectrum of **7b** in C_6D_6.

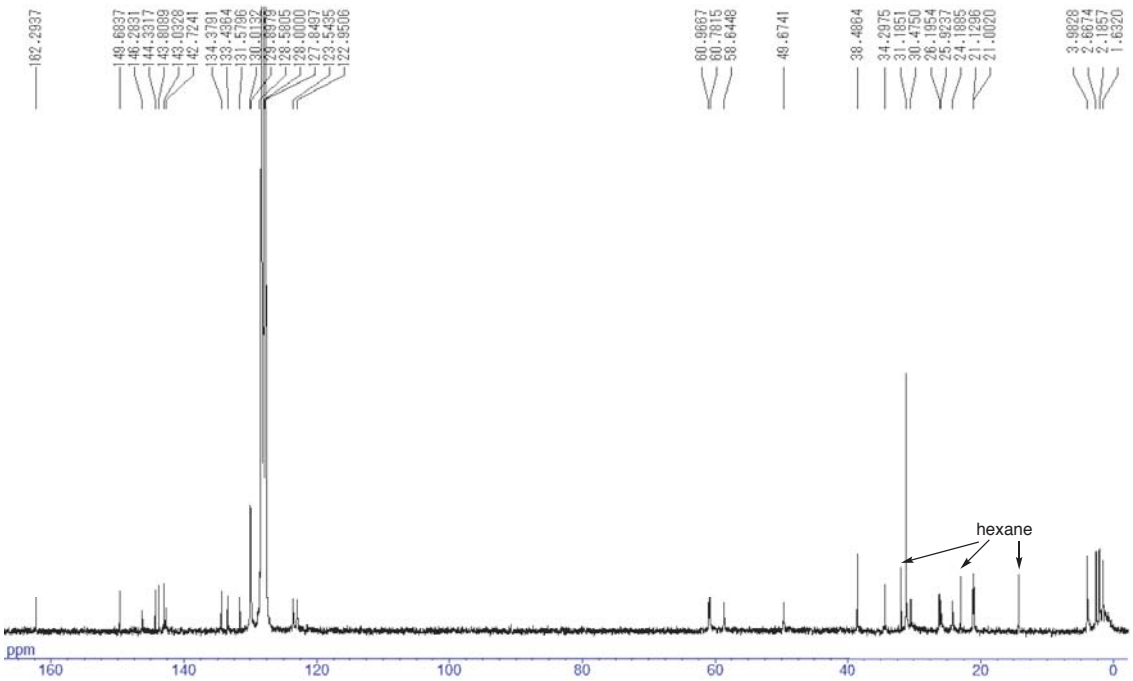

Figure S10. ^{13}C NMR spectrum of **7b** in C_6D_6.

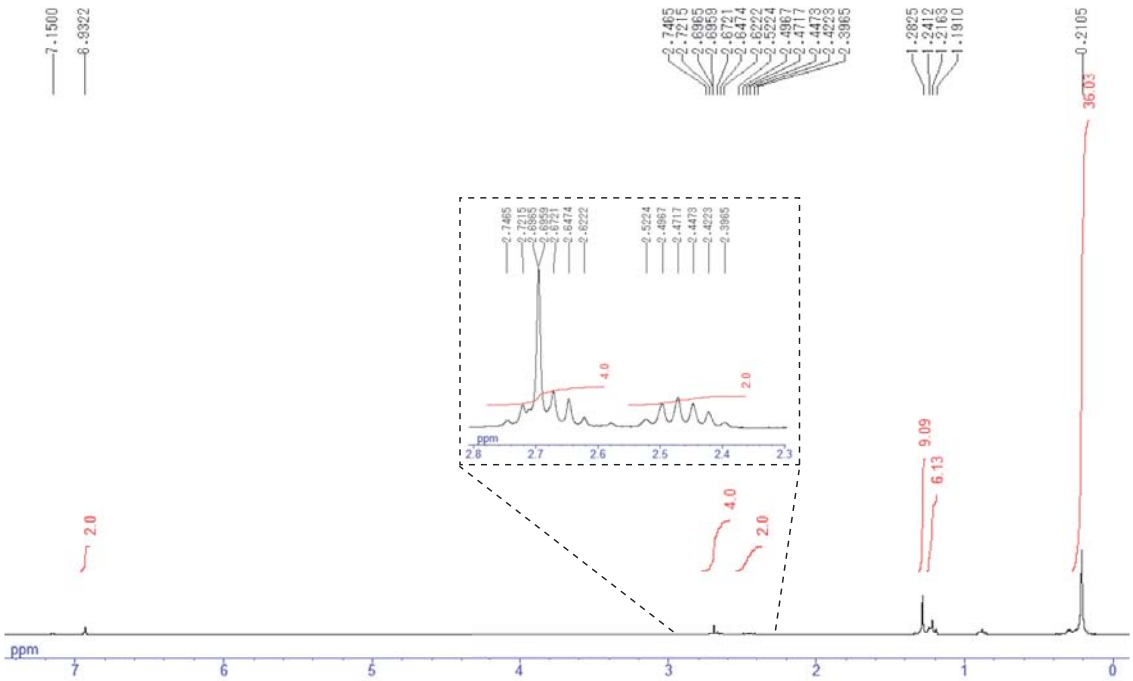

Figure S11. ^{1}H NMR spectrum of **14** in C_6D_6.

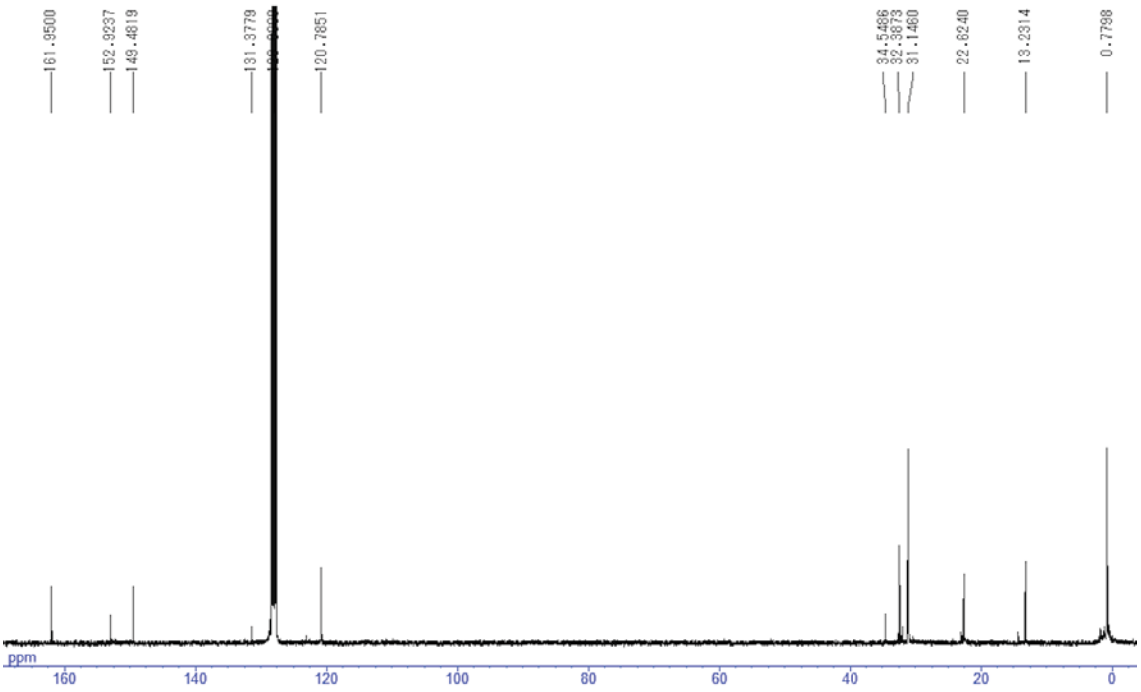

Figure S12. ^{13}C NMR spectrum of **14** in C_6D_6.

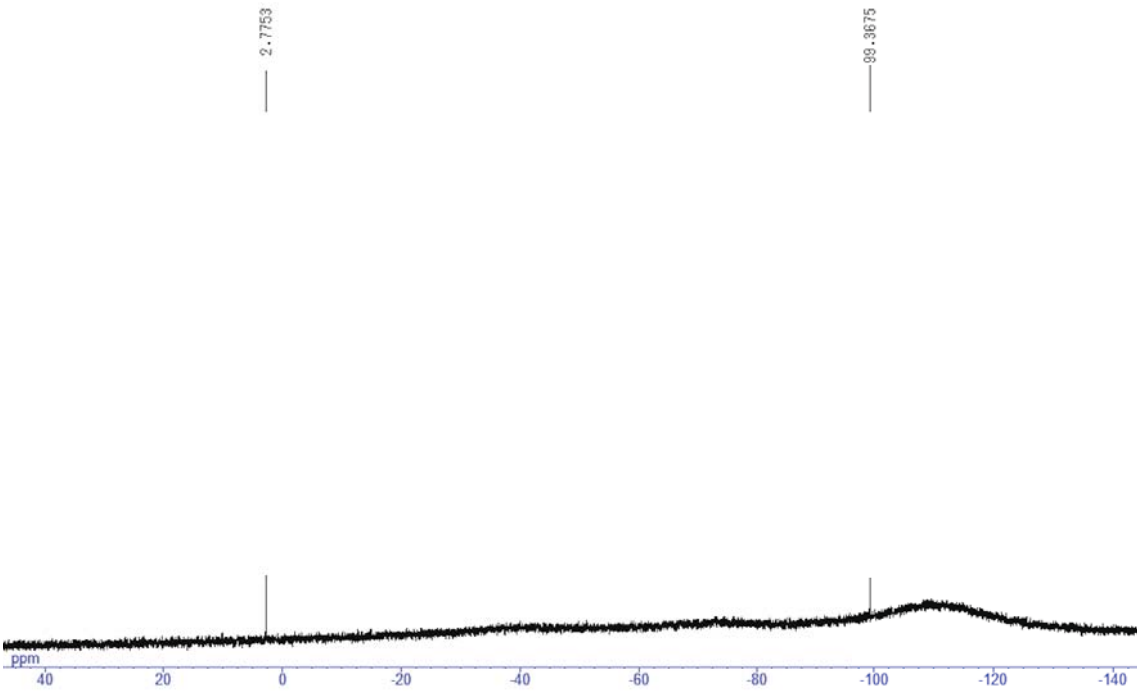

Figure S13. ^{29}Si NMR spectrum of **4** in C_6D_6.

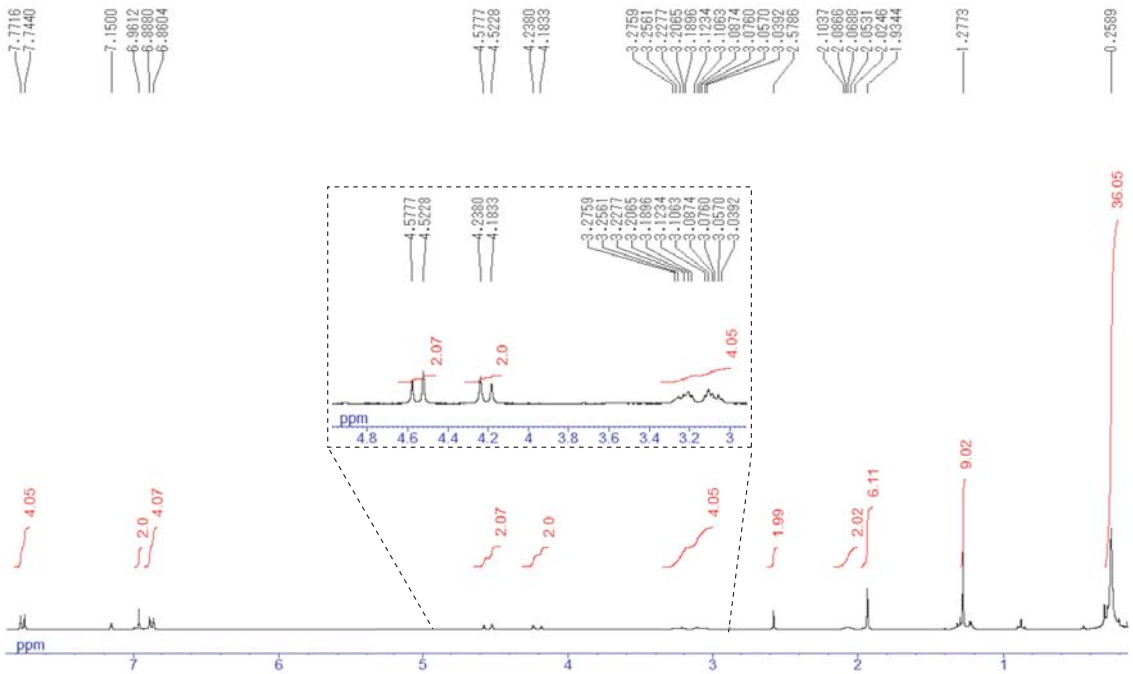

Figure S14. ^{1}H NMR spectrum of **16** in C_6D_6.

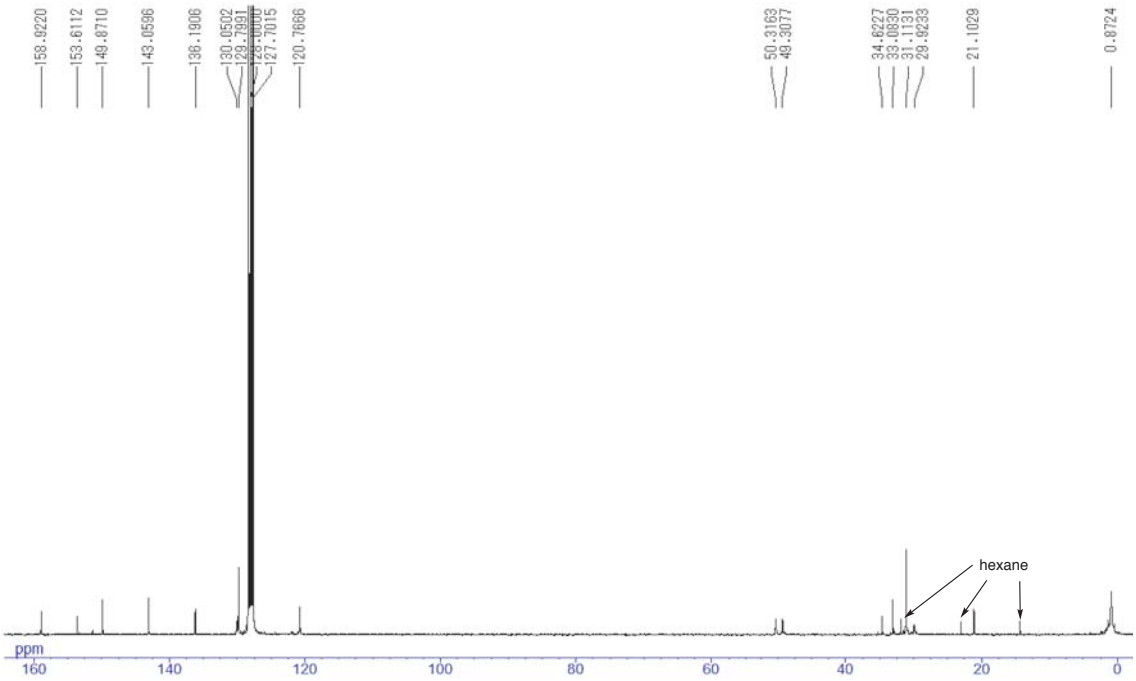

Figure S15. ^{13}C NMR spectrum of **16** in C_6D_6.

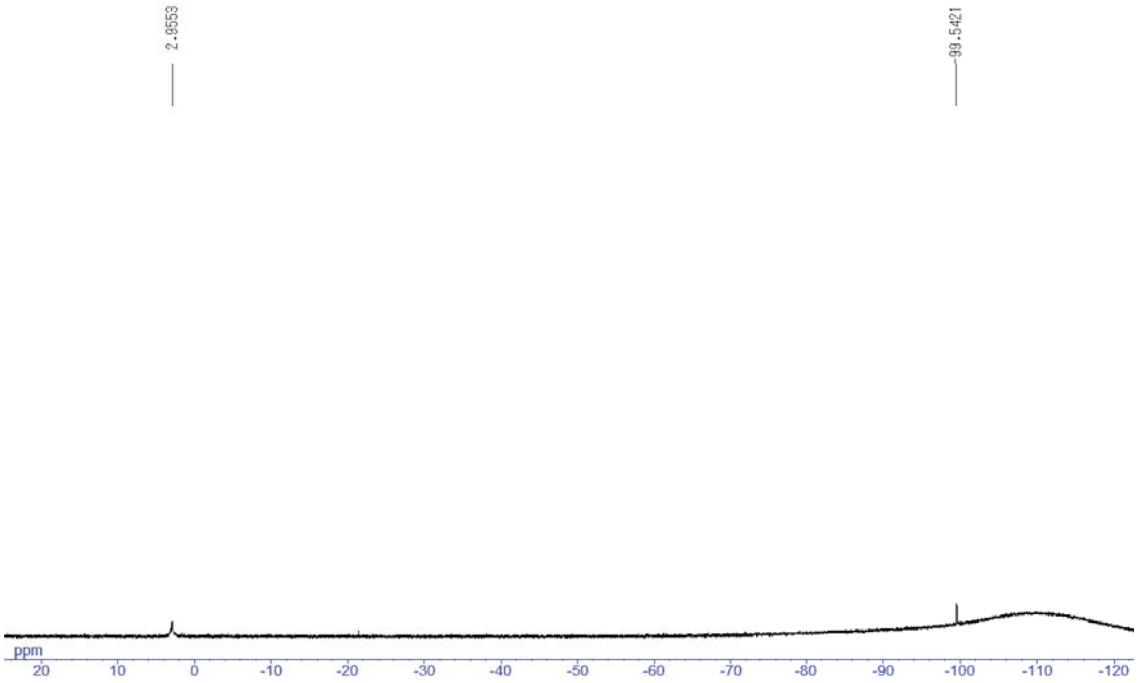

Figure S16. ^{29}Si NMR spectrum of **16** in C_6D_6.

3. X-Ray crystallographic analysis

Single crystals of **3**, [**6b**•2(C_6H_6)], [**7a**•0.5(C_6H_6)], [**7b**•0.5(C_6H_6)], **14** and **16** were obtained from recrystallization in *n*-hexane (**3**, **14**, **16**) and benzene (**6b**, **7a**, **7b**) at room temperature in an argon-filled glove box. Intensity data were collected on a RIGAKU Saturn70 CCD system with VariMax Mo Optic using MoK$_\alpha$ radiation (λ = 0.71073). Crystal data of **3** are shown in Figure 2 and reference 23. The structures were solved using a direct method (SHELXT[S4]) and refined by a full-matrix least-squares method on F^2 for all reflections using the programs of SHELXL-2014.[S5] All hydrogen atoms were placed using AFIX instructions, while all other atoms were refined anisotropically. Some preliminary diffraction data were collected and analyzed at the BL40XU/BL02B1 beamline of SPring-8 (2017B1726, 2017B1179, 2017B1193, 2018A1167, 2018B1668, 2018B1179, 2019A1057, 2019A1677, 2019B1129, 2019B1784) on a large cylindrical camera using synchrotron radiation (λ = 0.78255 Å).Supplementary crystallographic data were deposited at the Cambridge Crystallographic Data Centre (CCDC) under the numbers CCDC-1907434-1907439 and can be obtained free of charge from *via* www.ccdc.cam.ac.uk/data_request.cif. The authors greatly appreciate the kind help/suggestions of the reviewer for the analyses.

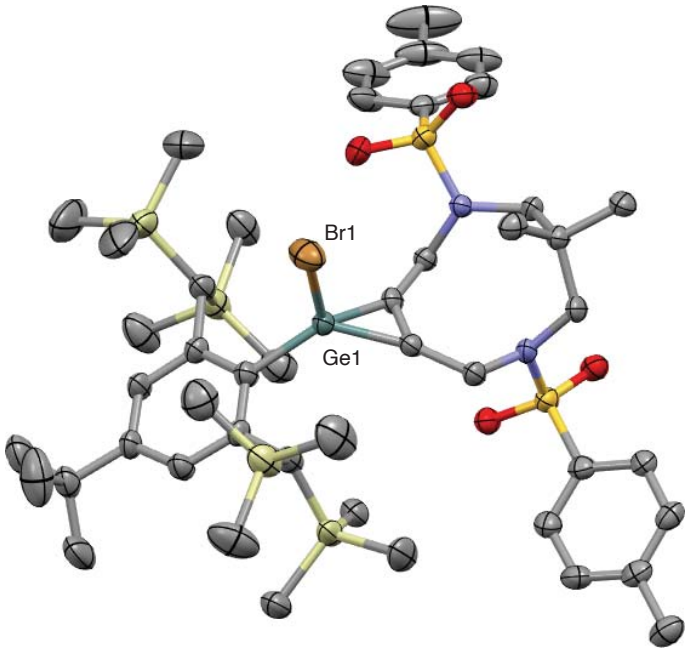

Figure S17. Molecular structure of [**6b**•2(C_6H_6)] (ORTEP; thermal ellipsoids set at 50% probability). Hydrogen atoms and two molecules of benzene were omitted for clarity.

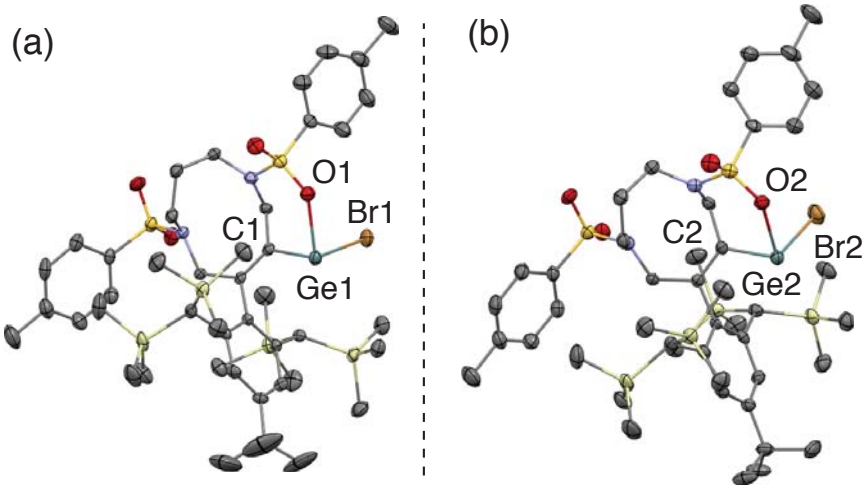

Figure S18. Molecular structure of [**7a**•0.5(C_6H_6)] (ORTEP; thermal ellipsoids set at 50% probability). Hydrogen atoms and one molecule of benzene were omitted for clarity. Two independent molecules are found in the unit cell ((a) molecule A, (b) molecule B).

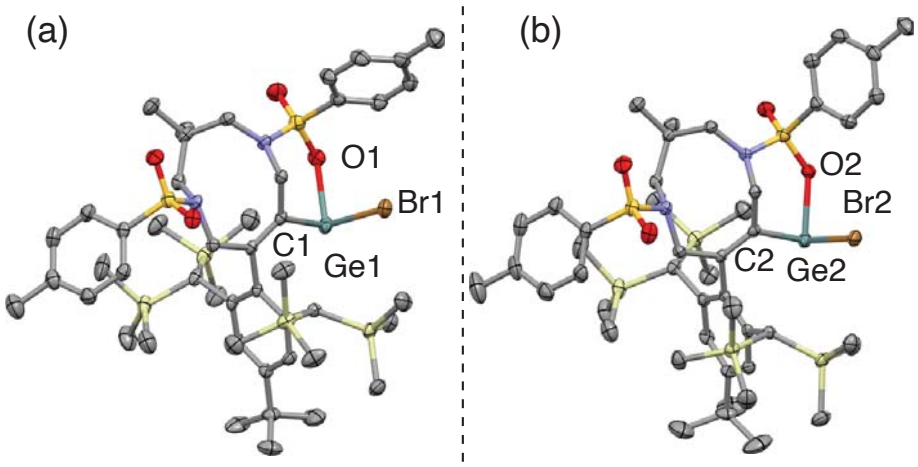

Figure S19. Molecular structure of [**7b**•0.5(C_6H_6)] (ORTEP; thermal ellipsoids set at 50% probability). Hydrogen atoms and one molecule of benzene were omitted for clarity. Two independent molecules are found in the unit cell ((a) molecule A, (b) molecule B).

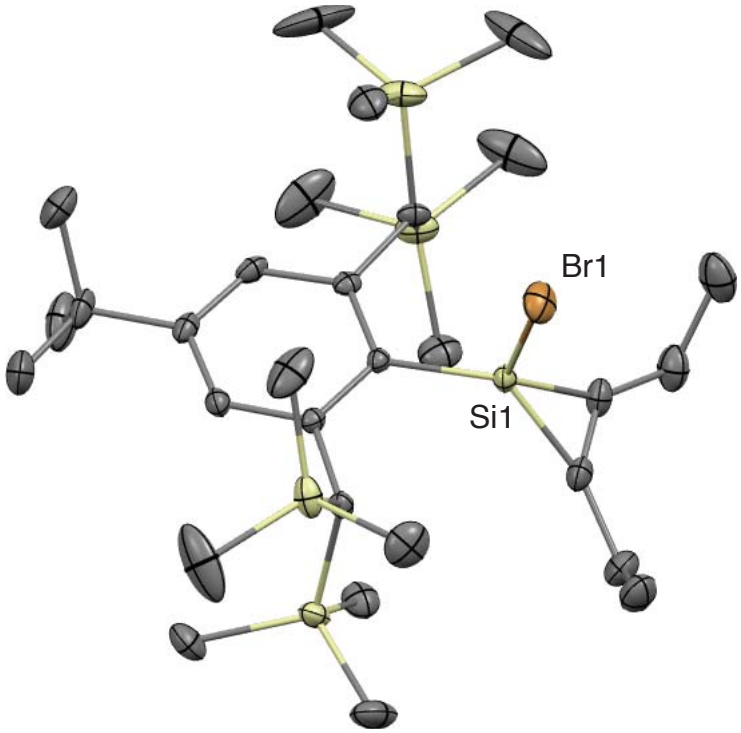

Figure S20. Molecular structure of **14** (ORTEP; thermal ellipsoids set at 50% probability). Hydrogen atoms were omitted for clarity.

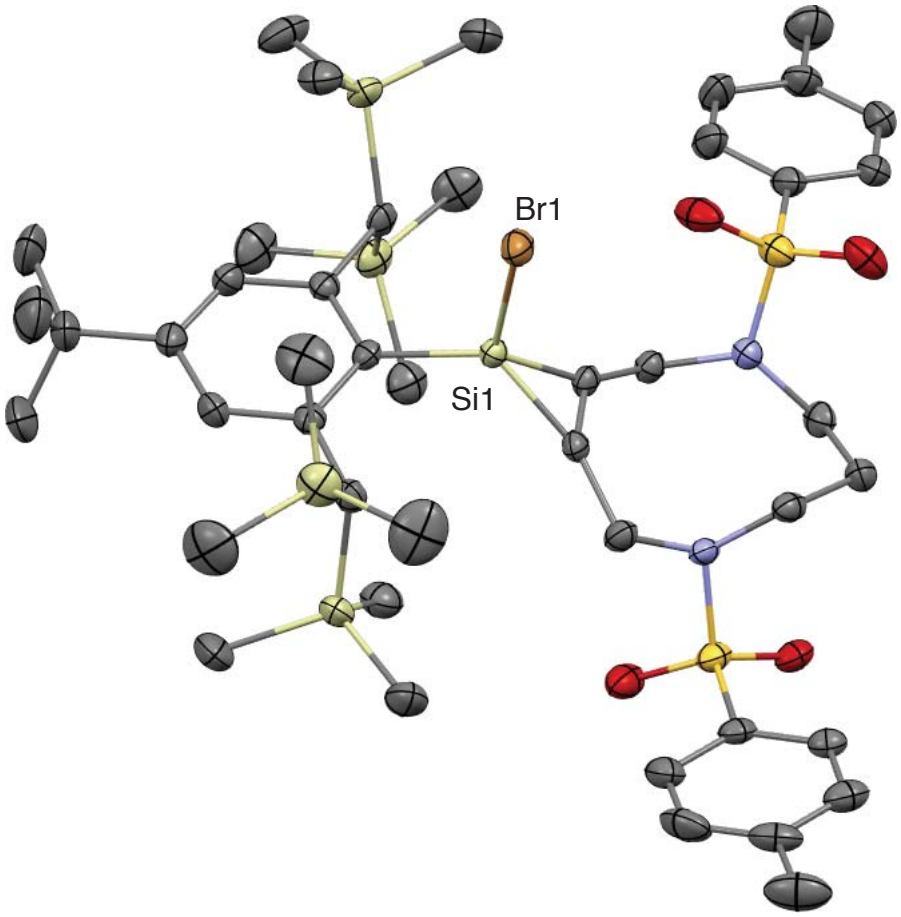

Figure S21. Molecular structure of **16** (ORTEP; thermal ellipsoids set at 50% probability). Hydrogen atoms were omitted for clarity.

Table S1. Crystal data and structural refinement data for [**6b**•1.204(C_6H_6)] and [**7a**•0.5(C_6H_6)].

Compound	[**6b**•1.204(C_6H_6)]	[**7a**•0.5(C_6H_6)]
Formula	$C_{54.22}H_{84.22}BrGeN_2O_4S_2Si_4$	$C_{48}H_{76}$ $BrGeN_2O_4S_2Si_4$
Molecular Weight	1157.07	1074.08
Temperature / ºC	–170	–100
λ (Å)	0.71073	0.71073
Crystal size / mm^3	0.08 x 0.05 x 0.02	0.11 x 0.08 x 0.03
Crystal system	triclinic	triclinic
Space group	*P*–1	*P*–1
a /Å	11.8162(2)	10.5431(2)
b /Å	12.9307(3)	20.8098(3)
c /Å	23.7235(6)	26.3903(4)
α / º	74.247(2)	76.5800(10)
β / º	88.954(2)	88.8460(10)
γ / º	65.242(2)	77.4580(10)
V /$Å^3$	3149.01(13)	5494.74(16)
Z	2	4
μ / mm^{-1}	1.304	1.489
$D_{calcd.}$ / $g \cdot cm^{-3}$	1.220	1.298
θ_{max}	25.500	28.366
Refl./restr./param.	11710/96/753	25416/3/1176
Completeness	99.7	92.4
GOF	1.087	1.016
R_1 (I>2σ(I))	0.0674	0.0558
wR_2 (I>2σ(I))	0.1639	0.1198
R_1 (all data)	0.0943	0.0932
wR_2 (all data)	0.1788	0.1344
Largest diff. peak and hole /$e \cdot Å^{-3}$	1.233, –0.712	1.205, –0.755
CCDC number	1907435	1907436

Table S2. Crystal data and structural refinement data for [**7b**•0.5(C_6H_6)]*, **14**, and **16**.

Compound	[**7b**•0.5(C_6H_6)]*	**14**	**16**
Formula	$C_{50}H_{80.06}Br_{0.94}GeN_2O_{4.06}S_2Si_4$	$C_{30}H_{59}BrSi_5$	$C_{45}H_{73}BrN_2O_4S_2Si_5$
Molecular	1098.36	640.13	990.53
Temperature / ºC	–100	–170	–170
λ (Å)	0.71073	0.71073	0.71073
Crystal size /	0.10 x 0.09 x 0.03	0.08 x 0.08 x 0.05	0.10 x 0.09 x 0.03
Crystal system	triclinic	monoclinic	monoclinic
Space group	*P*–1	$P2_1/n$	$P2_1/n$
a /Å	10.7385(1)	10.1417(2)	10.5503(5)
b /Å	20.7088(2)	16.7487(3)	20.8083(7)
c /Å	26.3913(3)	22.3189(4)	24.3847(9)
α / º	76.8720(10)	90	90
β / º	88.0890(10)	92.750(2)	93.320(3)
γ / º	78.7730(10)	90	90
V /Å^3	5605.81(10)	3786.73(12)	5344.3(4)
Z	4	4	4
μ / mm^{-1}	1.419	1.260	0.999
$D_{calcd.}$ / g·cm^{-3}	1.301	1.123	1.231
θ_{max}	28.348	28.366	25.492
Refl./restr./param	25803/12/1268	8790/0/342	9827/0/549
Completeness	92.0	92.6	98.8
GOF	1.018	1.022	1.052
R_1 (I>2σ(I))	0.0381	0.0372	0.0613
wR_2 (I>2σ(I))	0.0819	0.091	0.1464
R_1 (all data)	0.0598	0.0482	0.1052
wR_2 (all data)	0.0893	0.0956	0.1655
Largest diff. peak and hole	0.445, –0.361	0.956, –0.495	0.866, –0.970
CCDC number	1907437	1907438	1907439

*6% of hydrolyzed compound was contaminated as a minor disordered moiety.

4. Computational calculations

DFT calculations for model compounds (**1'**, **2'**, **3'**, **4'**, **8'**, **10'**, **11'**, **12'**, **13'**, **14'**, **15'**, **17'**, **18'**, **19'**, **20'**, **21'**, **2"**, **3"**, **4"**, **13"**, **14"**, **15"**, 1*H*–silirene, 1*H*-germirene, and the related species) were performed with the ORCA program.[S6] All geometry optimizations were run in redundant internal coordinates with tight convergence criteria using the B3LYP functional[S7] together with the def2-TZVP basis set.[S8] The 2010 Grimme's semiempirical atom-pair-wise London dispersion correction (DFT-D3) was included in all calculations.[S9] Harmonic frequency calculations verified the nature of ground or transition states having all positive or only one negative frequencies, respectively. From these optimized geometries all reported data were obtained by means of single-point (SP) calculations using the more polarized def2-TZVPP[S10] basis set. Energies were corrected for the zero-point energy (ZPE) term at the optimization level and computed by means of the recently developed near linear scaling domain-based local pair natural orbital (DLPNO) method[S11] to achieve coupled cluster theory with single-double and perturbative triple excitations (CCSD(T)).[S12] Except otherwise stated, solvent effects (toluene) were taken into account via the COSMO solvation model.[S13] Electric charges were computed using the Mulliken population analysis.[S14] Figure S22 was obtained with VMD.[S15]

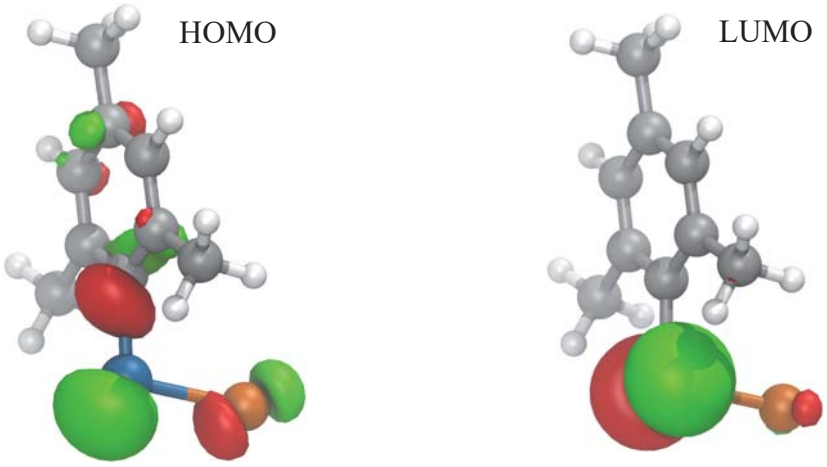

Figure S22. Kohn-Sham frontier molecular orbital isosurfaces (0.065 au isovalue) of **2"**.

PES for the reaction of 1'/12' with acetylene.

The possibility of an initial [2+2] cycloaddition between the digermene **1** with alkynes was thoroughly explored computationally by using the more simple *trans*-1,2-dimethyl-1,2-dibromo-digermene **1'** and acetylene (Scheme S1).

At the working level of theory ($COSMO_{tol}$/CCSD(T)/def2-TZVPP// $COSMO_{tol}$/B3LYP-D3/def2-TZVP), reaction of model digermene **1** with acetylene is highly exergonic (ΔE_{ZPE} = -49.60 kcal/mol) with a relatively low lying TS ($\Delta E^{\ddagger}_{ZPE}$ = 9.57 kcal/mol) (Figure S23). It is worth mentioning that Ge-Ge cleavage should be expected to have higher barrier, as deduced from the computed value ($\Delta E^{\ddagger}_{ZPE}$ = 18.70 kcal/mol) for the endergonic cleavage (ΔE_{ZPE} = 16.96 kcal/mol) of the larger model dimesityl-dibromo-digermene (**1''**) at the same level.

From the initially formed *cis*-1,2-dibromo-1,2-dimethyl-1,2-dihydro-1,2-di-germetene (*cis*-**8'**), elimination of a methylbromogermylene unit (**2**) and leading to the corresponding germirene **4'** turned out to be both kinetically ($\Delta E^{\ddagger}_{ZPE}$ = 57.39 kcal/mol) and thermodynamically (ΔE_{ZPE} = 54.99 kcal/mol) hampered. The comparatively favoured ($\Delta E^{\ddagger}_{ZPE}$ = 36.45 kcal/mol; ΔE_{ZPE} = 18.08 kcal/mol) Ge-Ge bond cleavage from *cis*-**8'** furnishes the product of simultaneous bromine atom migration between the two germanium centres **A'** (not shown in Figure S23). A different stereochemical approach for the Ge-insertion of **2'** into de Ge-C bond of germirene **4'** lead to the slightly more stable digermetene *trans* isomer (*trans*-**8'**), whose extrusion of acetylene occurs with [1,2]-bromine shift to give the new germirene **C'** via germylene **B'** (Scheme S1, Figure S23(a)). For the sake of comparison, chelotropic cycloaddition of germylene **2"** and acetylene to give germirene **4"** is an exergonic ($\Delta E^{\ddagger}_{ZPE}$ = -10.15 kcal/mol) low-barrier ($\Delta E^{\ddagger}_{ZPE}$ = 5.15 kcal/mol) reaction at the same level.

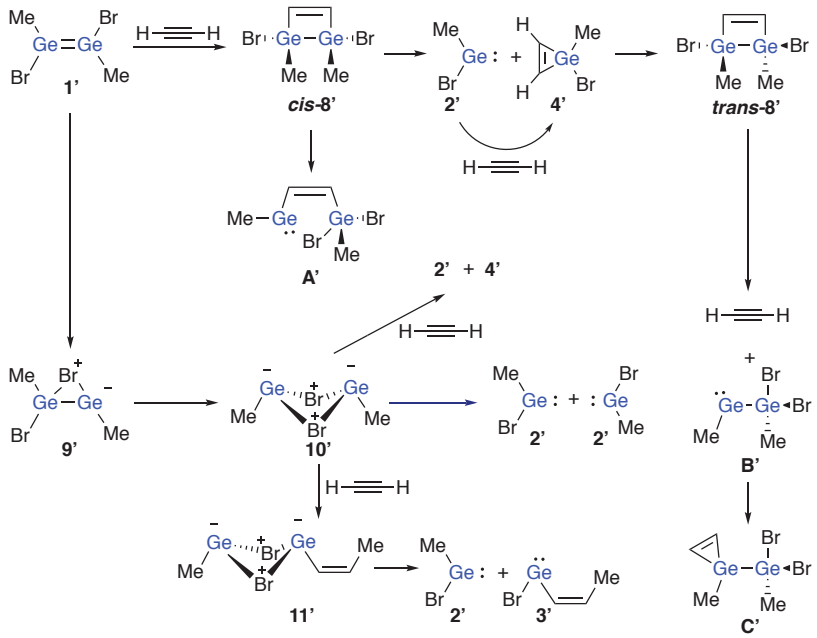

Scheme S1. Model reactions of digermene **1'** with acetylene.

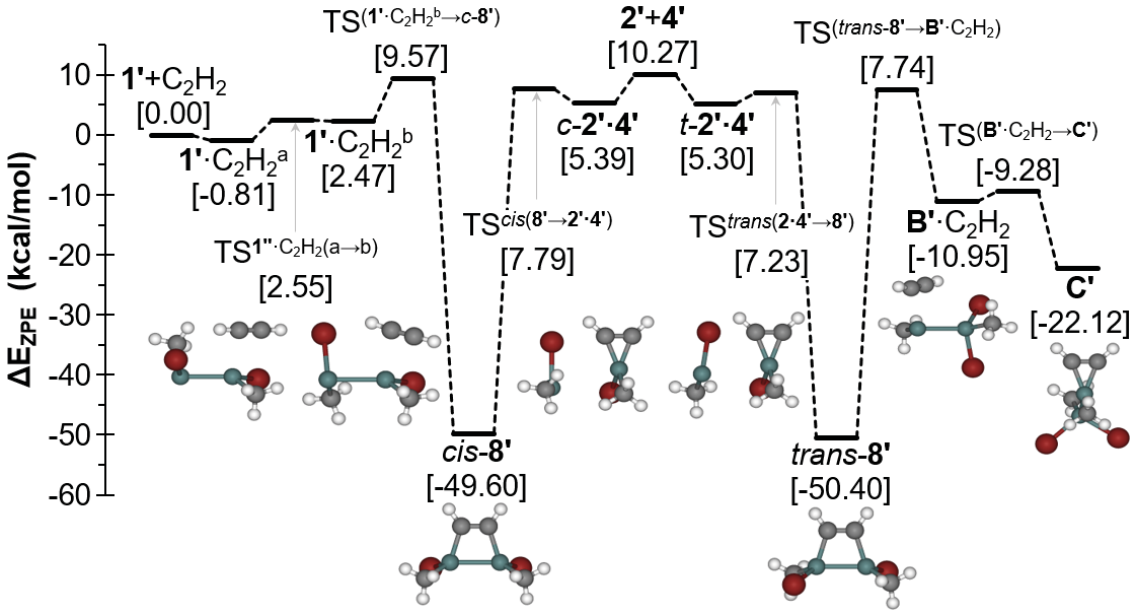

Figure S23. Computed ($COSMO_{tol}$/CCSD(T)/def2-TZVPP//$COSMO_{tol}$/B3LYP-D3/def2-TZVP) ZPE-corrected relative energies for the PES of model digermene **1'** + acetylene system.

An alternative to the dissociation of dibromodigermene **1'** into two bromogermylene units prior to reaction with acetylene reagents entails the initial conversion into di(μ^2-bromo)digermylene **10'**, that has been originally studied for the dimethyl substituted derivative **1'** (Scheme S1). The transformation occurs by sequential approach of every bromine atom to the originally nonbonded germanium centre in a two-step process through intermediate **9'**. The first step takes place through a low-lying transition state (TS) and is slightly exergonic (Figure S24). Compound **10'** can split endergonically (ΔE_{ZPE} = 20.42 kcal/mol relative to the reference digermene **1'**) in a barrierless process affording two units of bromogermylene **2'**. From these results it can be concluded that dibromodigermene **1'** should preferentially exist as the zwitterionic digermabromirane **9'** that could, in turn, serve as source for bromogermylene **2'**. Intermediate **9'** features a typical Ge-Ge single bond distance (2.528 Å),[S16] with Mayer Bond Order[S17] MBO = 0.793, in between that of the formal double bond in **1'** (2.441 Å; MBO = 1.159) and the formally non-bonded Ge atoms in **10'** (3.591 Å; MBO < 0.1). The exocyclic Ge-Br bond (2.373 Å; MBO = 0.898) is shorter than the endocyclic bond of Br to the neutral Ge1 atom (2.552 Å; MBO = 0.638) and the later in turn is shorter than that to the anionic Ge2 centre (2.762 Å; MBO = 0.460). The Ge-Br distances in the dibridged derivative **10'** (average 2.655 Å; MBO = 0.541) is half-way between the two Ge-Br endocyclic bonds in **9'**.

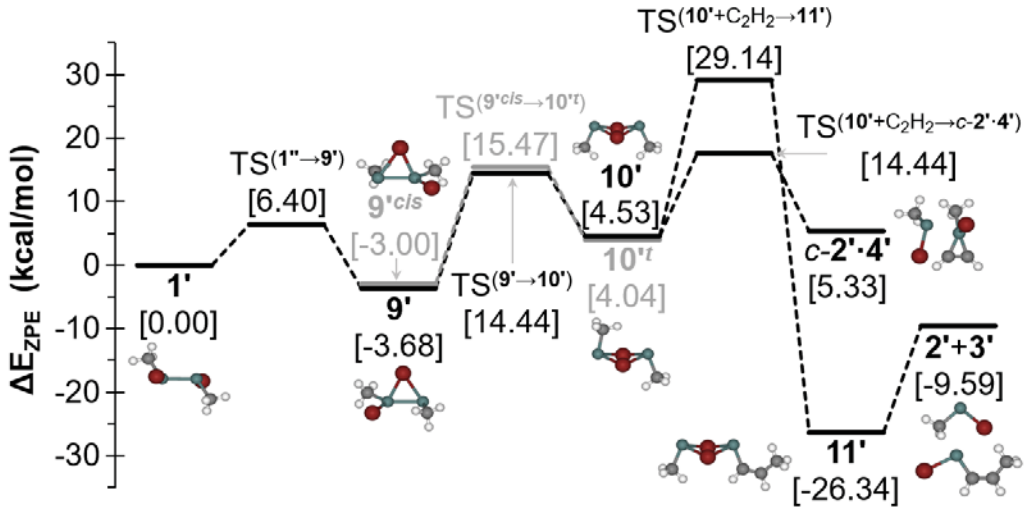

Figure S24. Computed ($COSMO_{THF}$/DLPNO-CCSD(T)/def2-TZVPP) zero-point corrected energy profile for the transformation of dimethyldibromodigermene **1'** into the products of formal chelotropic addition and Ge-C insertion of acetylene.

Alternatively, **10'** can react with acetylene yielding the chelotropic addition compound **4'**, as kinetic control product (with loss of a bromogermylene unit **2'**), or the thermodynamic control product **11'** by Ge-C insertion which, as in the case of **10'**, can split endergonically and without barrier to the final insertion product **3'**, with loss of **2'**.

The only isomer of Me-GeBr=GeBr-Me (**1'**) with Me-GeBr$_2$-Ge-Me structure (**1'iso**) was found as a van der Waals complex with acetylene (**1'iso**·C_2H_2) and was formed from cleavage of digermacyclobutene (**8'**). However, removal of acetylene from the above van der Waals complex leads to zwitterionic bromadigermirane (**9'**), which leads to the conclusion that **1'iso** (structure **B'** in Scheme S1) is not an energy minimum, at least for these dimethyl-substituted model species.

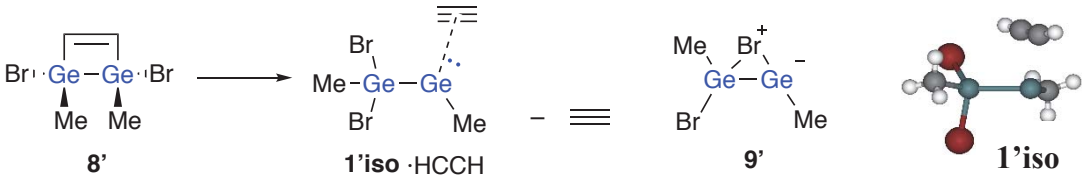

Compound **8'** leads endergonically ($\Delta\Delta E_{ZPE}$ = 18.08 kcal/mol) to *Z*-Me-Ge-CH=CH-GeBr$_2$-Me (**8'iso**) in a kinetically hampered process ($\Delta\Delta E_{ZPE}^{\ddagger}$ = 36.45 kcal/mol). This compound is partially stabilized by intramolecular Ge···Br interaction (d = 2.797 Å; compare with covalent Ge-Br bond distances 2.347 and 2.396 Å in the same compound).

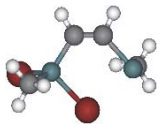
8'iso

Opposite to the Ge model case **1'**, reaction of model dibromo-dimethyl-disilene **12'** with acetylene does not follow a concerted [2+2] cycloaddition pathway but leads to the same very stable *cis*-1,2-dibromo-1,2-dimethyl-1,2-disilacyclobutene **17'** through low-lying zwitterionic intermediate **18'** and involving rather low barriers (Scheme S2). However, no TS could be found for the very endergonic cleavage of **17'** into bromosilylene **13'** and bromosilirene **14'**. These products can be alternatively formed via isomerization of disilene **12'** to di(μ^2-bromo)disilylene **20'**, that occur directly but not through a zwitterionic bromadisilirane intermediate **19'**, and low-barrier reaction with acetylene (Scheme S2). Again, opposite to the behaviour of the germa-analogue **10'**, the di(μ^2-bromo)disilylene **20'** does not undergo acetylene insertion into one of the C-Si bonds to give **21'**, but instead affords the cleavage products **13'** and **15'**. The endergonic splitting of **20'** into two bromosilylene units **13'** occurs in an almost barrierless process.[S18]

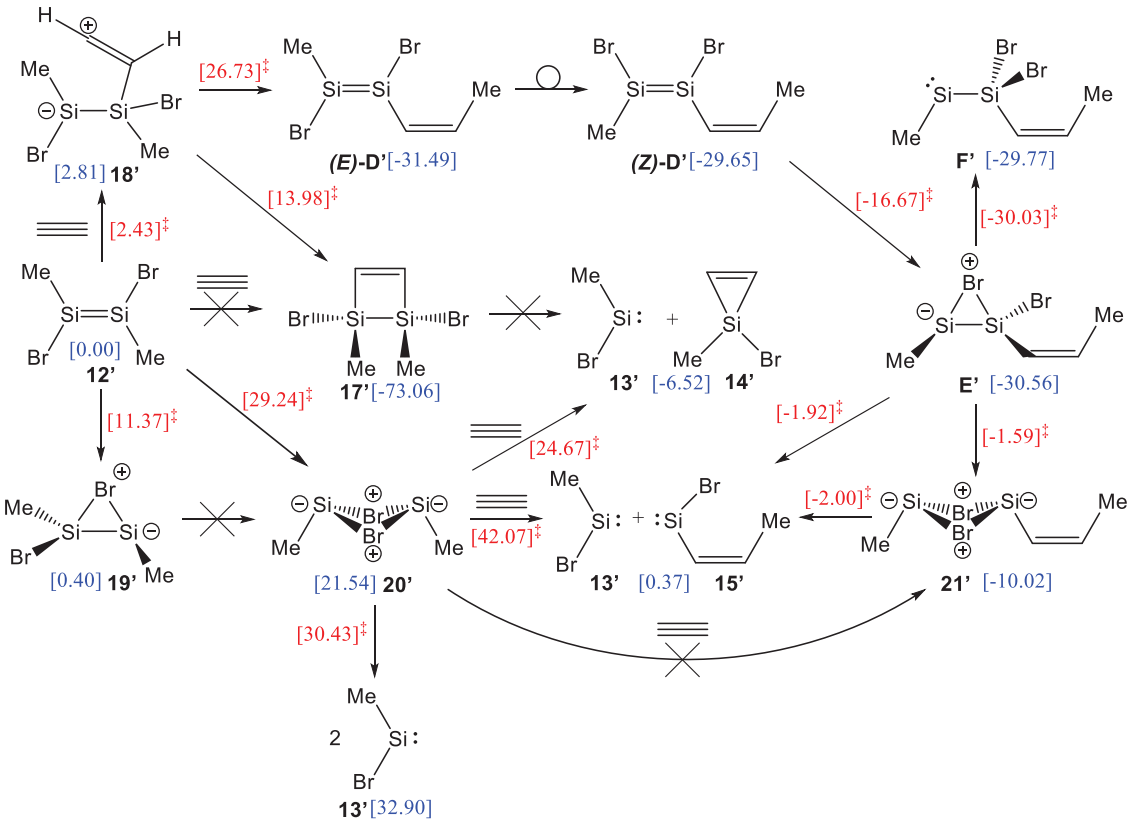

Scheme S2. Model reactions of disilene **12'** with acetylene.

A kinetically unfavoured pathway from the (methyl-substituted) model intermediate **18'**, but very likely favoured in more heavily-substituted derivatives, consists of the silicon-to-carbon [1,3] methyl group-migration leading to *E*-configured Si-C acetylene insertion product ***(E)*-D'**. Facile rotation around the Si=Si bond (reported in the general range 25.4-31.3 kcal/mol[S19] or even below 15 kcal/mol for tetrasilyl-substituted derivatives[S20]) forms diatereomer ***(Z)*-D'** which can undergo two-step bromine migration to compound **F'** via cyclic zwitterionic intermediate **E'**. The latter can easily afford **13'** and **14'** either directly or through the otherwise unreachable intermediate **21'**.

Ring strain energies (RSE) computed for parent 1*H*-silirene and 1*H*-germirene and their 1-bromosubstituted derivatives

The strain energies of the investigated unsaturated three-membered rings were calculated using homodesmotic reactions. The homodesmotic reactions (reaction class 4, or "RC4") are the second to last type in a hierarchy of increasingly more accurate processes, due to conservation of larger fragments, according to a recent classification and redefinition of the types of reaction used in thermochemistry.[S21] In this hierarchy, hyperhomodesmotic reactions (reaction class 5 or "RC5") constitute the type of processes of highest quality and precision, although the very small differences often found between RSE obtained with RC4 and RC5 reactions make homodesmotic reactions a reliable accurate option. They are defined to keep in reagents and products the same number of H_nX-YH_m bonds (X, Y are the two linked atoms, "n" and "m" are the number of H atoms attached to them), for each type of single, double or triple bond, as well as the same number of sp^3, sp^2 or unhybridized atoms of each element with 0, 1, 2 or three H atoms attached. The reaction schemes used for the evaluation of the RSE in parent (R = H) and 1-bromosubstituted (R = Br) 1*H*-tetrelirenes (E = Si, Ge) are displayed in Scheme S3 Where appropriate, C=C double bonds in cleavage products where set in *Z*-configuration by analogy of the *Z*-configured unsaturation in the cyclic species. RSE are then evaluated in the gas-phase at the working CCSD(T)/def2-TZVPP//B3LYP-D3/def2-TZVP level, as the average of the opposite values of the energetics (ΔE_{ZPE}) of the three endocyclic bond cleavage reactions (two of them being identical), the resulting values being collected in table S3.

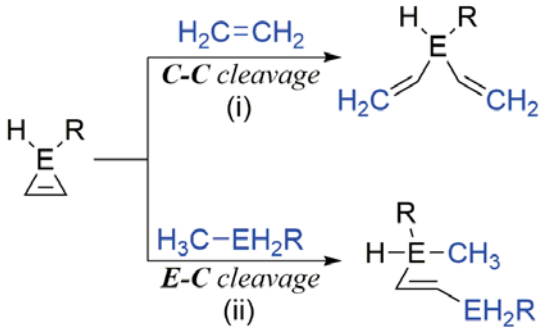

Scheme S3. Homodesmotic reactions used for the evaluation of RSE.

Table S3. Computed (CCSD(T)/def2-TZVPP//B3LYP-D3/def2-TZVP) RSE (kcal/mol) for parent and 1-bromosubstituted 1*H*-tetrelirenes, according to the homodesmotic (RC4) reactions displayed in Scheme S3.

E	R	RSE_{RC4}
Si	H	40.6
Si	Br	42.0
Ge	H	44.4
Ge	Br	47.6

From these results it can be concluded that i) RSE of 1*H*-gemirenes is higher (*ca.* 4-6 kcal/mol) than that of 1*H*-silirenes and ii) 1-bromosubstitution increases RSE by *ca.* 1 or 3 kcal/mol for 1*H*-silirenes or 1*H*-germirenes, respectively.

Calculations in real compounds

All calculations for the geometry optimization and frequency calculations of real models **2–4** were carried out on the *Gaussian 09* (Revision E.01) program package.[S22] The levels of theory used for the calculation were shown in the text. The frequency calculations confirmed minimum energies for the optimized structures.

・Geometry parameters and NBO analysis of Compound 3 at TPSSTPSS-D3(BJ)/6-311+G(2d,p)//TPSSTPSS-D3(BJ)/3-21G*[Ge,Si], 6-31G(d) [C,H,Br] level of theory.

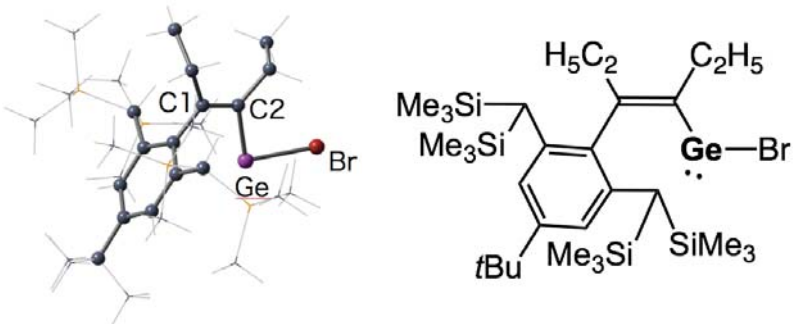

Figure S25. Optimized geometry of compound **3**.

Table S4. Selected optimized geometry parameters and results of NBO analysis of **3**.

	X-ray structure	Optimized model	Optimized model
	Selected geometry parameters		**WBIs**
Ge–Br /Å	2.417(2)	2.433	0.84
Ge–C2 /Å	1.9819(14)	2.016	0.69
C2–Ge–Br /º	99.80(5)	97.4	----
	Occupation number of electrons		
LP (Ge)	1.97 ($sp^{0.12}$)		
LP* (Ge)	0.27 (p orbital)		
LP-1 (Br)	1.99 ($sp^{0.32}$)		
LP-2 (Br)	1.97 ($sp^{46.53}$)		
LP-3 (Br)	1.88 (p orbital)		
π (Ge–C2)	1.87 (Ge, C2 p orbitals)		
	Second order perturbation theory analysis		
LP(Br)→LP*(Ge)	15.2 kcal/mol		
π (C1–C2)→LP*(Ge)	10.7 kcal/mol		

· Geometry parameters and NBO analysis of Compound 7a at TPSSTPSS-D3(BJ)/6-311+G(2d,p)//TPSSTPSS-D3(BJ)/3-21G*[Ge,Si], 6-31G(d) [other] level of theory.

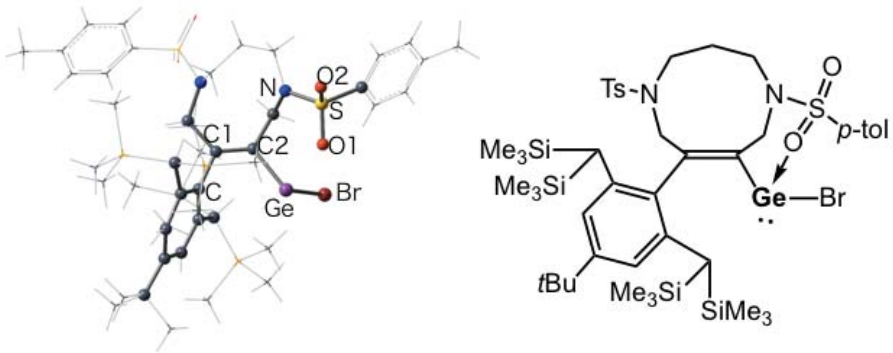

Figure S26. Optimized geometry of compound **7a**.

Table S5. Selected optimized geometry parameters and results of NBO analysis of **7a**.

	X-ray structure	Optimized model	Optimized model
	Selected geometry parameters		**WBIs**
Ge–Br /Å	2.4315(6) 2.4286(5)	2.485	0.71
Ge–C2 /Å	1.997(4) 2.002(3)	2.015	0.64
Ge–O1 /Å	2.231(3) 2.203(3)	2.213	0.22
C2–Ge–Br /º	96.41(9) 95.81(9)	93.9	----
	Second order perturbation theory analysis		
LP(Br)→LP*(Ge)	9.1, 37.1, 149.4 kcal/mol		
π (C1–C2)→LP*(Ge)	3.1, 3.6 kcal/mol		
LP(O1)→LP*(Ge)	77.6 kcal/mol		

• Geometry parameters and NBO analysis of Compound 7b at TPSSTPSS-D3(BJ)/6-311+G(2d,p)//TPSSTPSS-D3(BJ)/3-21G*[Ge,Si], 6-31G(d) [other] level of theory.

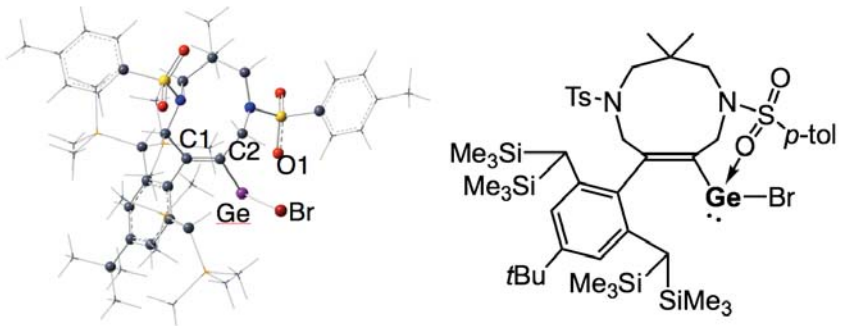

Figure S27. Optimized geometry of compound **7b.**

Table S6. Selected optimized geometry parameters and results of NBO analysis of **7b**.

	X-ray structure	Optimized model	Optimized model
	Selected geometry parameters		**WBIs**
Ge–Br /Å	2.4310(4) 2.4290(4)	2.483	0.71
Ge–C2 /Å	2.005(3) 1.999(2)	2.014	0.63
Ge–O1 /Å	2.228(2) 2.214(2)	2.237	0.21
C2–Ge–Br /º	96.98(7) 95.46(7)	93.4	----
	Second order perturbation theory analysis		
LP(Br)→LP*(Ge)	9.2, 37.4, 149.0 kcal/mol		
π (C1–C2)→LP*(Ge)	2.7, 4.1 kcal/mol		
LP(O1)→LP*(Ge)	75.9 kcal/mol		

• Mechanism for the reaction between 2 and 3-hexyne to furnish bromovinylgermylene 3

The mechanism of the reaction between bromogermylene **2** and 3-hexyne to afford bromovinylgermylene **3** should be similar to that between **2”** and HCCH, which affords **3”** and **4”** as kinetic and thermodynamic product, respectively.

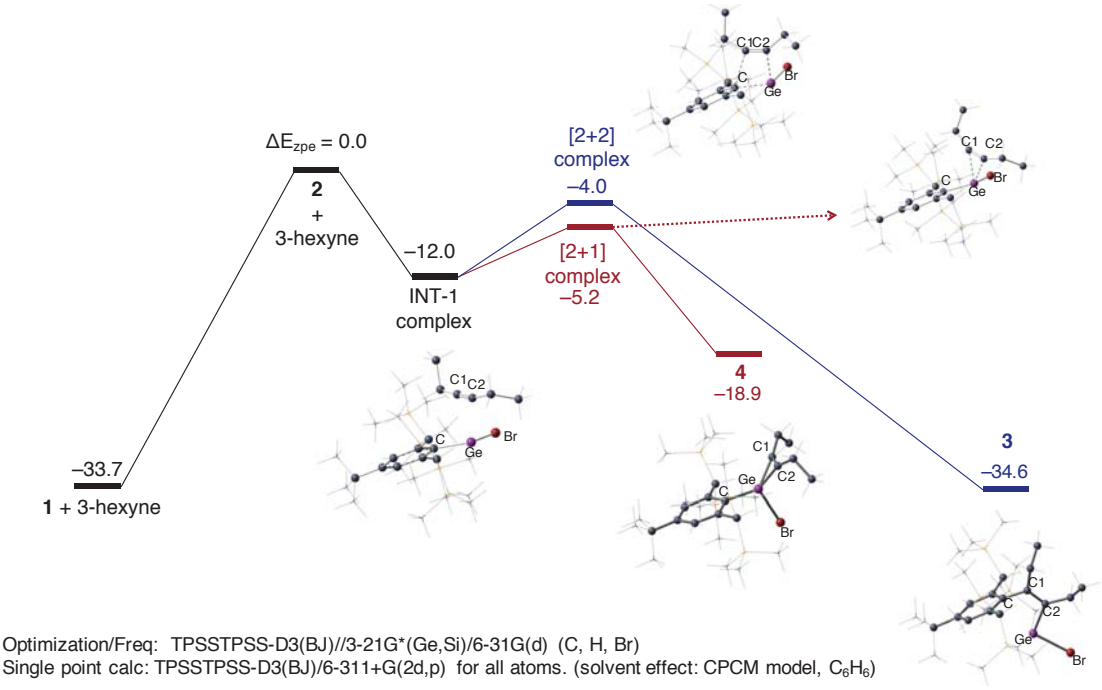

Optimization/Freq: TPSSTPSS-D3(BJ)//3-21G*(Ge,Si)/6-31G(d) (C, H, Br)
Single point calc: TPSSTPSS-D3(BJ)/6-311+G(2d,p) for all atoms. (solvent effect: CPCM model, C_6H_6)

Figure S28. Calculated pathways from bromogermylene **2** to **3** or **4** (in kcal/mol).

5. References

S1) Pangborn, A. B.; Giardello, M. A.; Grubbs, R. H.; Rosen, R. K.; Timmers, F. J., *Organometallics* **1996**, *15*, 1518-1520.

S2) (a) Sasamori, T.; Sugahara, T.; Agou, T.; Guo, J.-D.; Nagase, S.; Streubel, R. Tokitoh, N., *Organometallics*, **2015**, *34*, 2106-2109. (b) Sugahara, T.; Guo, J.-D.; Sasamori, T.; Karatsu, Y.; Furukawa, Y.; Ferao, A. E.; Nagase, S.; Tokitoh, N., *Bull. Chem. Soc. Jpn.* **2016**, *89*, 1375-1384. (c) R. Ni, N. Mitsuda, T. Kashiwagi, K. Igawa, K. Tomooka, *Angew. Chem. Int. Ed.* **2015**, *54*, 1190. (d) K. Igawa, S. Aoyama, Y. Kawasaki, T. Kashiwagi, Y. Seto, R. Ni, N. Mitsuda, K. Tomooka, *Synlett* **2017**, *28*, 2110. (e) T. Sugahara, J.-D. Guo, D. Hashizume, T. Sasamori, S. Nagase, N. Tokitoh, *Dalton Trans.* **2018**, *47*, 13318.

S3) Sugahara, T.; Guo, J.-D. Sugahara, T. *et al.* Reaction of a stable digermyne with acetylenes: synthesis of a 1,2-digermabenzene and a 1,4-digermabarrelene. *Bull. Chem. Soc. Jpn.* **89**, 1375-1384 (2016).

S4) Sheldrick, G. M. A short history of *SHELX*. *Acta Cryst.* **A64**, 112–122 (2008).

S5) Sheldrick, G. M. SHELXT - Integrated space-group and crystal-structure determination. *Acta Cryst.* **A71**, 3-8 (2015).

S6) ORCA - An *ab initio*, DFT and semiempirical SCF-MO package. Written by F. Neese, Max Planck Institute for Bioinorganic Chemistry, D-45470 Mülheim/Ruhr, 2012. Version 3.0.3. Web page: http://www.cec.mpg.de/forum/portal.php. F. Neese, *WIREs Comput Mol Sci* **2012**, *2*, 73–78.

S7) a) A. D. Becke, *J. Chem. Phys.,* **1993**, *98*, 5648-5652. b) C. T. Lee, W. T. Yang, R. G. Parr, *Phys. Rev. B,* **1988**, *37*, 785-789.

S8) F. Weigend, R. Ahlrichs, Phys. *Chem. Chem. Phys.* **2005**, *7*, 3297-3305.

S9) S. Grimme, J. Antony, S. Ehrlich, H. Krieg, *J. Chem. Phys.* **2010**, *132*, 154104.

S10) A. Bergner, M. Dolg, W. Kuchle, H. Stoll, H. Preuss, *Mol. Phys.* **1993**, *80*, 1431 − 1441. Obtained from the EMSL Basis Set Library at https://bse.pnl.gov/bse/portal. D. Feller, *J. Comp. Chem.*, **1996**, *17*, 1571-1586.

S11) C. Riplinger, B. Sandhoefer, A. Hansen, F. Neese, *J. Chem. Phys.* **2013**, *139*, 134101-134113.

S12) J. A. Pople, M. Head-Gordon, K. Raghavachari, *J. Chem. Phys.* **1987**, *87*, 5968–5975.

S13) a) A. Klamt, G. Schüürmann, *J. Chem. Soc. Perkin Trans. 2,* **1993**, *220*, 799-805; b) A. Klamt, *J. Phys. Chem.* **1995**, *99*, 2224-2235.

S14) R. S. Mulliken, "Electronic population analysis on LCAO–MO molecular wave functions. I" *J. Chem. Phys.*, **1955**, *23*, 1833-1840, DOI: 10.1063/1.1740588.

S15) VMD — Visual Molecular Dynamics. W. Humphrey, A. Dalke, K. Schulten, "VMD: Visual molecular dynamics" *J. Molec. Graphics*, **1996**, *14*, 33-38, DOI: 10.1016/0263-7855(96)00018-5. (http://www.ks.uiuc.edu/Research/ vmd/)

S16) A reference of experimental Ge-Ge single bond distances must be provided here and/or, alternatively, the computed distances for model H_3Ge-GeH_3 (2.436 Å) and $H_2Ge{=}GeH_2$ (2.301 Å) at the same level.

S17) (a) Mayer, I. Charge, bond order and valence in the AB initio SCF theory. *Chem. Phys. Lett.*, **1983**, *97*, 270-274, DOI 10.1016/0009-2614(83)80005-0. (b) Mayer, I. Bond order and valence: Relations to Mulliken's population analysis. *Int. J. Quant. Chem.*, **1984**, *26*, 151-154, DOI 10.1002/qua.560260111. (c) Mayer, I. Bond orders and valences in the SCF theory: a comment. *Theor. Chim. Acta*, **1985**, *67*, 315-322, DOI 10.1007/BF00529303. (d) Mayer, I. In *Modelling of Structure and Properties of Molecules*, Maksic, Z. B. (Ed.), John Wiley & sons, New York, Chichester, Brisbane, Toronto, **1987**. (e) Bridgeman, A. J.; Cavigliasso, G.; Ireland, L. R.; Rothery, J. The Mayer bond order as a tool in inorganic chemistry. *J. Chem. Soc., Dalton Trans.*, **2001**, 2095-2108, DOI 10.1039/B102094N.

S18) The TS for the **20'**→2·**13'** step is lower in energy than the two **13'** molecules due to the fact that the product lacks the stabilizing noncovalent interaction energy in the preliminary formed van der Waals complex and also due to the correction energy terms at the final CCSD(T) level (at the optimization level the TS is just 0.20 kcal/mol higher than the **13'·13'** van der Waals complex).

S19) V. Y. Lee, A. Sekiguchi, in *Organometallic Compounds of Low-Coordinate Si, Ge, Sn and Pb: From Phantom Species to Stable Compounds*, John Wiley & Sons Ltd., Chichester, United Kingdom, **2010**, p53.

S20) M. Kira, S. Ohya, T. Iwamoto, M. Ichinohe, C. Kabuto, *Organometallics*, **2000**, *19*, 1817-1819.

S21) a) S. E. Wheeler, K. N. Houk, P. v. R. Schleyer, W. D. Allen, *J. Am. Chem. Soc.* **2009**, *131*, 2547–2560; b) A. Rey, A. Espinosa Ferao, R. Streubel, *Molecules*, **2018**, *23*, 3341

S22) Gaussian 09, Revision E.01, Frisch, M. J., Trucks, G. W., Schlegel, H. B., Scuseria, G. E., Robb, M. A., Cheeseman, J. R., Scalmani, G., Barone, V., Mennucci, B. G., Petersson, A., Nakatsuji, H., Caricato, M., Li, X., Hratchian, H. P., Izmaylov, A. F., Bloino, J., Zheng, G., Sonnenberg, J. L., Hada, M., Ehara, M., Toyota, K., Fukuda, R., Hasegawa, J., Ishida, M., Nakajima, T., Honda, Y., Kitao, O., Nakai, H., Vreven, T., Montgomery, Jr., J. A., Peralta, J. E., Ogliaro, F., Bearpark, M., Heyd, J. J., Brothers, E., Kudin, K. N., Staroverov, V. N., Keith, T., Kobayashi, R., Normand, J., Raghavachari, K., Rendell, A., Burant, J. C., Iyengar, S. S., Tomasi, J., Cossi, M., Rega, N., Millam, J. M., Klene, M., Knox, J. E., Cross, J. B., Bakken, V., Adamo, C., Jaramillo, J., Gomperts, R., Stratmann, R. E., Yazyev, O., Austin, A. J., Cammi, R., Pomelli, C., Ochterski, J. W., Martin, R. L., Morokuma, K., Zakrzewski, V. G., Voth, G. A., Salvador, P., Dannenberg, J. J., Dapprich, S., Daniels, A. D., Farkas, O., Foresman, J. B., Ortiz, J. V., Cioslowski, J. & Fox, D. J. Gaussian, Inc., Wallingford CT, **2013**.